NUREG/IA-0215
NSI RRC KI 90-12/01-03-07

International Agreement Report

Spatial Effects and Uncertainty Analysis for Rod Ejection Accidents in a PWR

Prepared by:
A. Avvakumov, V. Malofeev, V. Sidorov

Nuclear Safety Institute
Russian Research Centre
"Kurchatov Institute"
1, Kurchatov Sq., Moscow
123182 Russia

H. H. Scott, NRC Project Manager

Office of Nuclear Regulatory Research
U.S. Nuclear Regulatory Commission
Washington, DC 20555-0001

September 2007

Prepared for
U.S. Nuclear Regulatory Commission, Institute for Radioprotection and Nuclear Safety (France),
and Ministry of Science and Technologies of the Russian Federation

Published by
U.S. Nuclear Regulatory Commission

AVAILABILITY OF REFERENCE MATERIALS IN NRC PUBLICATIONS

NRC Reference Material

As of November 1999, you may electronically access NUREG-series publications and other NRC records at NRC's Public Electronic Reading Room at http://www.nrc.gov/reading-rm.html. Publicly released records include, to name a few, NUREG-series publications; *Federal Register* notices; applicant, licensee, and vendor documents and correspondence; NRC correspondence and internal memoranda; bulletins and information notices; inspection and investigative reports; licensee event reports; and Commission papers and their attachments.

NRC publications in the NUREG series, NRC regulations, and *Title 10, Energy*, in the Code of *Federal Regulations* may also be purchased from one of these two sources.

1. The Superintendent of Documents
   U.S. Government Printing Office
   Mail Stop SSOP
   Washington, DC 20402–0001
   Internet: bookstore.gpo.gov
   Telephone: 202-512-1800
   Fax: 202-512-2250
2. The National Technical Information Service
   Springfield, VA 22161–0002
   www.ntis.gov
   1–800–553–6847 or, locally, 703–605–6000

A single copy of each NRC draft report for comment is available free, to the extent of supply, upon written request as follows:

Address: U.S. Nuclear Regulatory Commission
Office of Administration
Mail, Distribution and Messenger Team
Washington, DC 20555-0001
E-mail: DISTRIBUTION@nrc.gov
Facsimile: 301–415–2289

Some publications in the NUREG series that are posted at NRC's Web site address http://www.nrc.gov/reading-rm/doc-collections/nuregs are updated periodically and may differ from the last printed version. Although references to material found on a Web site bear the date the material was accessed, the material available on the date cited may subsequently be removed from the site.

Non-NRC Reference Material

Documents available from public and special technical libraries include all open literature items, such as books, journal articles, and transactions, *Federal Register* notices, Federal and State legislation, and congressional reports. Such documents as theses, dissertations, foreign reports and translations, and non-NRC conference proceedings may be purchased from their sponsoring organization.

Copies of industry codes and standards used in a substantive manner in the NRC regulatory process are maintained at—

The NRC Technical Library
Two White Flint North
11545 Rockville Pike
Rockville, MD 20852–2738

These standards are available in the library for reference use by the public. Codes and standards are usually copyrighted and may be purchased from the originating organization or, if they are American National Standards, from—

American National Standards Institute
11 West 42nd Street
New York, NY 10036–8002
www.ansi.org
212–642–4900

Legally binding regulatory requirements are stated only in laws; NRC regulations; licenses, including technical specifications; or orders, not in NUREG-series publications. The views expressed in contractor-prepared publications in this series are not necessarily those of the NRC.

The NUREG series comprises (1) technical and administrative reports and books prepared by the staff (NUREG–XXXX) or agency contractors (NUREG/CR–XXXX), (2) proceedings of conferences (NUREG/CP–XXXX), (3) reports resulting from international agreements (NUREG/IA–XXXX), (4) brochures (NUREG/BR–XXXX), and (5) compilations of legal decisions and orders of the Commission and Atomic and Safety Licensing Boards and of Directors' decisions under Section 2.206 of NRC's regulations (NUREG–0750).

NUREG/IA-0215
NSI RRC KI 90-12/01-03-07

International Agreement Report

Spatial Effects and Uncertainty Analysis for Rod Ejection Accidents in a PWR

Prepared by:
A. Avvakumov, V. Malofeev, V. Sidorov

Nuclear Safety Institute
Russian Research Centre
“Kurchatov Institute”
1, Kurchatov Sq., Moscow
123182 Russia

H. H. Scott, NRC Project Manager

Office of Nuclear Regulatory Research
U.S. Nuclear Regulatory Commission
Washington, DC 20555-0001

September 2007

Prepared for
U.S. Nuclear Regulatory Commission, Institute for Radioprotection and Nuclear Safety (France),
and Ministry of Science and Technologies of the Russian Federation

Published by
U.S. Nuclear Regulatory Commission

ABSTRACT

A rod ejection accident is a design-basis event for a pressurized water reactor. It is well known that spatial effects play a very important role in this accident. In this study four cases using a model of Three Mile Island Unit 1 are considered: ejection of the central or peripheral control rod at the end of cycle or the beginning of cycle. Calculations were carried out using the BARS neutronic code coupled with the RELAP5/MOD3.2 thermal hydraulic code. This coupled code allows three-dimensional pin-by-pin neutronics and assembly-by-assembly thermal-hydraulics simulation of a transient. The results showed that the major parameters of the accident (the peak power and core energy deposition) were a function of spatial effects. Analysis of the dependence of the peak local fuel enthalpy on spatial effects was performed. Uncertainty analysis was carried out for the central control rod ejection accident at hot zero power conditions. The analysis of uncertainties was performed for the following parameters: local fuel enthalpy, maximum core power, and power pulse width. Calculated results showed that the uncertainty in key safety parameters would be determined to a great extent by the uncertainty in the control rod worth. The effect of initial core power on the above parameters was analyzed using a rod ejection accident starting from 33% of rated power.

FOREWORD

Regulatory agencies in most countries require licensees to routinely analyze postulated reactivity-initiated accidents, and fuel damage criteria are established to assess the consequences of those accidents. At the time that high burnup was shown to affect such damage criteria, representatives from the Kurchatov Institute in Russia informed several research organizations that the Kurchatov Institute had performed related tests with high-burnup fuel, but the test results had not been evaluated. Subsequently, cooperative arrangements were made between the Kurchatov Institute, the French Institute for Radiological Protection and Nuclear Safety (IRSN, formerly IPSN), and the U.S. Nuclear Regulatory Commission to evaluate the test results. Those results have now been evaluated, supplemented, and published in two NUREG/IA reports (0156 and 0213).

Although the test reactor data were the main interest of the collaboration, there was also interest in examining best-estimate methods available in Russia for plant safety analyses as a means of comparing code capabilities. This was especially interesting because the Russian neutron kinetics code, BARS, had a completely different developmental history than the codes being used in France and the U.S. Examination of the Russian code was accomplished by analyzing several postulated reactivity transients. The present report describes all of the BARS calculations for rod-ejection accidents in a PWR with UO_2 fuel. Three other related reports are in preparation, discussing computations for boron-dilution accidents with UO_2 fuel, rod-ejection accidents with mixed-oxide (MOX) fuel, and other related benchmarks.

Brian W. Sheron, Director
Office of Nuclear Regulatory Research
U.S. Nuclear Regulatory Commission

CONTENTS

Appendices

LIST OF FIGURES

LIST OF TABLES

EXECUTIVE SUMMARY

This study was undertaken to analyze spatial effects in the course of rod ejection accidents. If the rod worth is sufficient to reach prompt critical i.e. greater than β, then its withdrawal initiates a fast power excursion which is terminated due to the negative reactivity feedback. This event is of interest from the point of view of prediction of the maximum increase in fuel enthalpy during the accident. Although, as numerous steady-state calculations show, the maximum value of control rod worth scarcely exceeds 1β in a PWR, such an accident is to be considered in a NPP safety analysis with conservatively increased value of the ejected rod worth.

A key parameter of interest in a NPP safety analysis is the peak local fuel enthalpy, which establishes the acceptance criterion for unacceptable fuel damage in reactivity initiated accidents in a LWR. It is well-established that spatial effects play an important role in the REA consequences, in particular, the core peak power and energy deposition which can be approximately related to the fuel enthalpy rise under an adiabatic assumption (no heat transfer from the fuel to the coolant). Then using simplified analytical approximations it is easy to establish relationships between the major parameters of interest and spatial effects. An influence of spatial effects on the REA parameters is revealed in two opposite trends. On the one hand, the higher the power peaking factor, the higher the local fuel enthalpy. On the other hand, a higher value of the power peaking factor tends to slow down the total energy deposition in the core and, as a result, to mitigate the fuel enthalpy increase. This is due to the fact that the fuel and moderator feedback is stronger in the hottest regions of the reactor core and reduces the peak power and reactivity.

In this study an analysis of REAs was carried out using the RELAP–BARS code, which allows a 3-D pin-by-pin neutronic and assembly-by-assembly thermal-hydraulic simulation of a LWR. Four REAs with ejection of the central or peripheral control rod at the EOC or BOC initial conditions were analyzed using a PWR calculational model based on TMI-1. To provide identical initial conditions the worth of an ejected control rod was artificially fitted to 1.21β for all cases. The calculational results showed that the peak powers were different to a great extent: from 4.4 to 37.5 GW. In the cases with ejection of the peripheral rod, the peak power was lower compared with ejection of the central rod by 2.5 times at EOC and by 2.9 times at BOC. In turn, practically the same, but inverse relationship was found for the power peaking factors. The maximum fuel enthalpy increase was about 26 cal/g at BOC and 17-19 cal/g at EOC. From the point of view of the assembly-by-assembly representation, the central rod ejection accidents with rather small power peaking factors resulted in slightly higher values of the maximum fuel enthalpy increase. On the contrary, the pin-by-pin representation showed that the peak local fuel enthalpy was higher for the peripheral REAs with the highest power peaking factors. In the EOC cases, a higher value of the peak enthalpy was due to the fact that the hottest fuel pin was found in an assembly diagonally adjacent to the hot assembly. This fact indicates that a problem of proper definition of the hottest pin location is essential. In the considered case the incorrect definition of the hottest pin location using an assembly-by-assembly approach, can lead to 15%-underestimation in the peak local enthalpy rise.

The point kinetics approximation within the Nordheim-Fuchs model allowed to derive simple relationship between the peak power, total energy deposition and the power peaking factor. It was found that in the framework of this model the peak power and total energy deposition are inversely proportional to the power peaking factor. Thus, if the peaking factor for fuel enthalpy increase is approximately the same as that for power, then it can be expected that the maximum assembly-average fuel enthalpy increase is practically independent on spatial effects.

Another important problem of a REA analysis deals with uncertainty in prediction of the rod worth by different calculational methods. As was found during this study, the BARS results for the rod worths were always higher compared with those calculated by the PARCS code. The most difference occurs for the peripheral rod nearest to the reflector region. At the EOC initial conditions this difference reaches 35%.

The uncertainty analysis for the PWR central rod ejection accident starting from the HZP conditions carried out with the RALAP-BARS code showed that the uncertainties in the key parameters of the accident would be determined to a great extent by the uncertainty in ejected rod worth. For a rod worth of 1.2β with the uncertainty of 15% (corresponding to two standard deviations), the uncertainty in local fuel enthalpy was estimated as 110%, the uncertainty in the maximum core power – as 216%, and the uncertainty in power pulse width – as 76%. The results demonstrated non-adiabatic nature of the transient and showed that the sensitivity of fuel enthalpy to the most of neutronic and thermal-hydraulic quantities strongly depends on time. Qualitatively, the RELAP-BARS results are agreed with the PARCS ones.

The comparative study of the accident starting from 33% of rated power showed strong dependence of a number of the REA parameters on initial core power. Under the same rod worth of 1.2β, the peak power in the transient from 33% of rated power was by 3.5 times greater than that in the transient from HZP. Unlike the HZP case, a change in the hottest fuel pin location takes place due to power redistribution during the transient from the non-zero power. This phenomenon can lead to some difficulties to predict the hottest pin using assembly-by-assembly approach together with the pin reconstruction procedure to calculate fuel pellet enthalpy. In comparison with the HZP case, the REA from 33% of rated power leads to the increase in the maximum fuel pellet enthalpy up to 67 cal/g.

In general, the conclusion was that the influence of spatial effects may be of interest not only in an analysis of reactivity initiated events, but also in interpretation of in-pile burst tests aimed to understand fuel rod behavior under severe accidents. The present study has also looked at the effect of the calculation approach (pin-by-pin against assembly-by-assembly) on the major parameter of a REA – the peak local enthalpy increase.

ACKNOWLEDGEMENTS

This work was performed at Russian Research Centre “Kurchatov Institute” as part of a project supported by the U.S. Nuclear Regulatory Commission (NRC), Institute for Radioprotection and Nuclear Safety (IRSN, France) and Ministry of Science and Technologies of the Russian Federation. The authors gratefully acknowledge Dr. David Diamond of Brookhaven National Laboratory (BNL, USA) for his work and leadership during the entire period of this project.

ABBREVIATIONS

BNL	Brookhaven National Laboratory (USA)
BOC	Beginning of Cycle
EOC	End of Cycle
FA	Fuel Assembly
HZP	Hot Zero Power
IRSN	Institute for Radioprotection and Nuclear Safety (France)
LWR	Light Water Reactor
NRC	Nuclear Regulatory Commission (USA)
NPP	Nuclear Power Plant
NSI	Nuclear Safety Institute
PWR	Pressurized Water Reactor
REA	Rod Ejection Accident
RRC KI	Russian Research Centre “Kurchatov Institute”
TMI-1	Three Mile Island Unit 1
1-D	One-Dimensional
2-D	Two-Dimensional
3-D	Three-Dimensional

1 INTRODUCTION

1.1 Background

The rod ejection accident (REA) is a design-basis reactivity initiated event for a pressurized water reactor (PWR). The rod ejection scenario assumes a mechanical failure of the control rod drive mechanism and, as a result, ejection of a control rod to a fully withdrawn position due to the reactor coolant system pressure. If the ejected rod worth is sufficient, a rapid power excursion occurs, which is terminated by the negative fuel temperature (Doppler) feedback within a few hundredths of a second.

From the point of view of a nuclear power plant safety analysis, peak local fuel enthalpy is a key parameter used as the acceptance criterion for fuel behavior in the course of reactivity initiated events in LWRs. It is clear that local fuel enthalpy depends on a spatial distribution of the energy deposition in the core during the accident; therefore, to determine a peak value of this parameter accurately, it is necessary to consider 3 D pin-by-pin neutronic model. In best-estimate nodal diffusion methods such a problem is usually split into two steps: first – a calculation of assembly-average power distribution, and second – peak power estimate within selected fuel assemblies by a pin-by-pin reconstruction method with further estimate of the peak local fuel enthalpy. This procedure has evident drawbacks compared with the direct pin-by-pin methods, especially when spatial effects are very complicated during the event.

Analysis of a REA, as a rule, involves the following parameters of interest: the core peak power and the energy deposition, which can be approximately related to the fuel enthalpy rise under the assumption of an adiabatic process (i.e. no heat transfer to the coolant). A simple analytical approximation, based on the Nordheim-Fuchs model, allows to establish dependence of the peak power, pulse width and energy deposition on several parameters: the inserted reactivity (rod worth), delayed neutron fraction, prompt neutron lifetime, and a parameter which characterizes the Doppler feedback. As it was found the magnitude of the last parameter depended strongly on spatial effects during a transient.

It is well-established that spatial effects play an important role in the REA consequences of interest. These effects are revealed in a dual manner. On the one hand, the higher the power peaking factor, the higher the local energy deposition and, consequently, the local fuel temperature (or enthalpy) increase. On the other hand, it is well-known that the Doppler feedback is stronger in the hottest fuel regions and reduces the peak power and reactivity. Besides, local heating of the coolant also decreases the peak power and reactivity.

The REA analyses were performed using the RELAP–BARS code (Ref. 1), which allows a 3-D pin-by-pin neutronics and assembly-by-assembly thermal-hydraulics simulation of a light water reactor (LWR). Calculations were carried out for four PWR REAs with ejection of the central or peripheral control rod at the end of cycle (EOC) or the beginning of cycle (BOC). To provide maximum non-uniformity of the power distribution in axial direction, all control rods were either fully inserted in the core or fully withdrawn during a transient.

As it was mentioned the most important safety parameter of reactivity initiated accident is maximum local fuel pellet enthalpy. 3-D best-estimate neutronics methods are available to calculate local fuel pellet enthalpy; but unlike 1-D or 2-D very conservative methodologies, these methods do not guarantee conservative estimation in key safety parameters during such an accident. Therefore, it is important to determine the uncertainty in fuel enthalpy calculated by a best-estimate code.

Recently a qualitative approach to an uncertainty analysis for the rod ejection accident (REA) was developed in Brookhaven National Laboratory (BNL, USA). For the REA, the fact that the physics of the transient is relatively well-known allowed the authors to define a simplified methodology to estimate the uncertainty in fuel enthalpy. The approach is based on using point kinetics in determining the quantities, which determine the uncertainty in fuel enthalpy instead of a very complicated consideration of uncertainties in cross sections.

The approach was applied to the uncertainty analysis of a PWR REA at hot zero power conditions (HZP). The analysis took into account the point kinetics parameters, which were obtained from 3-D calculations and engineering judgement as to the uncertainty in those parameters. The results showed that the uncertainty in local fuel enthalpy would be determined primarily by the uncertainty in ejected rod worth and delayed neutron fraction. For an uncertainty in the former of 8% (one standard deviation) and the latter of 5%, the uncertainty in fuel enthalpy was 51% for control rod worth of 1.2β (β – delayed neutron precursor fraction). However, the authors considered only a few quantities of interest and their analysis was based on a conservative adiabatic assumption for fuel temperature calculation.

1.2 Objectives

The objective of this study was to analyze spatial effects in the course of rod ejection accidents with withdrawal of the central or off-central control rod. A PWR calculational model has 1/8 radial symmetry and includes fuel assemblies with different properties surrounded by the radial reflector. In an axial direction a uniform core nodalization scheme (axial layers with different properties) is used with the top and bottom reflectors. Although the BARS code allows a continuous axial distribution of power (due to use of the Fourier series expansion), hereinafter an axial power distribution is given in terms of used nodalization scheme (for the simplicity in a code intercomparison).

In this study the following parameter is used to characterize spatial effects in the REAs: the total power peaking factor, F_q, defined as a ratio between the maximum fuel pellet power and an average pellet power over the core. It should be noted that “fuel pellet” term in this study is related to a calculational axial node, which is generally larger compared with the actual height of a fuel pellet. This definition of the power peaking factor is valid for the pin-by-pin approach. In an assembly-by-assembly representation the following definition of the power peaking factor, $F_q^{'}$, is used: it is a ratio between the maximum power in an axial node of the hottest assembly to an average node power (provided that uniform axial nodalization is used).

Another objective of this study is to analyze the uncertainty in peak fuel enthalpy, core power, and power pulse width for a REA in the TMI-1 PWR at HZP conditions. Sensitivity of these parameters to a variety of neutronic and thermal-hydraulic quantities of the core was studied using the pin-by-pin neutronic model together with more realistic thermal-hydraulic model that are implemented in the RELAP-BARS code. The effect of initial core power on key parameters of the accident was analyzed using calculational results for the TMI-1 REA starting from 33% of rated power.

1.3 Outline of Report

Section 2 focuses on the analysis of the RELAP–BARS calculational results for considered transients. This section also contains descriptions of the calculational models. The Nordheim-Fuchs model is used to understand the role of spatial effects on the major parameters of a REA. Evaluations of the feedback parameter as a function of the power peaking factor are derived. This section provides also a comparison of the rod worth steady-state calculations performed by different codes and possible uncertainties in the REA parameters due to uncertainty in the rod worth prediction.

Section 3 focuses on the uncertainty analysis for the central rod ejection accident. The methodology of the uncertainty analysis for the PWR REA is described. In Section 3 the uncertainty in the peak fuel enthalpy, core power, and power pulse width is assessed to a number of neutronic and thermal-hydraulic quantities. The effect of the initial core power on parameters of the accident is analyzed by a comparative study of the TMI-1 REA starting from 33% of rated power.

Appendix A contains the calculational results obtained by RELAP–BARS during modeling of a REA with ejection of the central rod with increased worth at EOC conditions.

2 SPATIAL EFFECTS FOR ROD EJECTION ACCIDENTS

2.1 RELAP-BARS Transient Calculations

The reactor model was based on Three Mile Island Unit 1 (TMI-1) used as an international benchmark exercise (Ref. 2). The reference design for the PWR is derived from the reactor geometry and operational data of the TMI-1 NPP. Two different cores were used in this study. First core is assumed to be at the end of cycle (EOC), with a boron concentration in the coolant of 5 ppm, and equilibrium Xe and Sm concentration. The average burnup in the core is 40.7 GWd/t (the maximum burnup is about 58 GWd/t). Detailed specifications for this core are given in Ref. 2. Another core is assumed to be at the beginning of cycle (BOC) with the average core exposure of 18.2 GWd/t and boron concentration of 1700 ppm (Ref.3). The hot zero power (HZP) conditions are defined as follows: the reactor power is 2772 W (10^{-6} of rated power), fuel/coolant temperature is 551 K and core inlet pressure is 15.4 MPa. The reactor has one-eight core symmetry, as Figures 2.1 and 2.2 show. Initial steady-states are the same for both cores: control rod banks 1 to 4 are completely withdrawn, banks 5 to 7 are completely inserted. Figures 2.1 and 2.2 show only inserted control rod banks. For the simplicity it was assumed that the delayed neutron fraction was 521.10 pcm at EOC and 632.34 pcm at BOC.

For the calculations, a control rod cluster of Bank 7 is ejected from the core centre (Assembly H8) or periphery (Assembly N12) during 0.1 s to initiate a transient. The calculations were continued for 2.5 seconds. This duration was chosen from the previous analysis of the rod ejection accidents where it was found that the fuel enthalpy increase has been arrested due to the reactor trip by that time (Ref. 4). In this study no reactor scram was assumed. Thus, four cases were studied: two types of REA (the central or peripheral rod ejection) at two initial conditions (EOC or BOC).

Steady-state calculations show that an actual worth of the ejected rod is lower compared with the delayed neutron fraction, β. Table 2.1 presents the calculational results obtained by the BARS code at EOC (Ref. 5) and BOC. It is obvious, that these magnitudes are insufficient to reach prompt critical. Since a power excursion below prompt critical is out of interest, the control rod worth in each case of this study was fixed at 1.21β. This worth is possible only when there is a large distortion of flux distribution over the core: for instance, if the control rod at position M11 is out of the core throughout the transient with ejection of the peripheral control rod at position N12. Thus, to provide 1.21β worth of the ejected rod, the initial core conditions have to be changed. In cases of the central rod ejection there were changes in neutronic parameters of the ejected rod. When the peripheral rod was ejected, the control rod in Assembly M11 was assumed to be stuck out of the core and the ejected rod was partly inserted to the core to provide required 1.21β worth.

Due to different delayed neutron fractions at EOC and BOC, an assumption of 1.21β worth means that the absolute value of the rod worth at BOC is greater by 21% compared with the EOC cases. For this reason it can be expected in this study that consequences of BOC REAs are to be more severe in terms of fuel enthalpy. (To compare the results for EOC REA with the same absolute value of the rod worth as at BOC, i.e. 1.47β, an additional calculation was carried out for the central rod ejection. The calculational results are given in Appendix A.)

	8	9	10	11	12	13	14	15
H	52.86 Bank 7	30.19	56.25	30.85	49.53 Bank 7	28.11	53.86 Bank 6	55.78
K		57.94	30.80	55.43	29.83	53.95 Bank 5	25.55	49.17
L			57.57 Bank 6	30.22	54.40	27.86	23.30	47.30
M				49.71 Bank 5	28.85	52.85	40.94	
N					48.75 Bank 7	23.86	41.45	
O						37.34		

52.86	- fuel burnup (GWd/t)
Bank 7	- No. of regulating bank

Figure 2.1. One-Eight Core Layout (EOC Initial Conditions)

	8	9	10	11	12	13	14	15
H	30.69 Bank 7	0.16 Gd + B	29.50	0.18 Gd + B	24.53 Bank 7	0.16 Gd + B	36.51 Bank 6	48.20
K		32.26	0.17 Gd + B	29.30	0.17 Gd + B	29.25 Bank 5	0.15 Gd + Gd	40.34
L			31.69 Bank 6	0.18 Gd + B	30.12	0.17 Gd + B	0.14	39.62
M				24.52 Bank 5	0.18 B	31.73	26.73	
N					24.89 Bank 7	0.17	32.22	
O						24.82		

30.69	- fuel burnup (GWd/t)
Bank 7	- No. of regulating bank

Gd	- 4 fuel pins with Gd
B	- B_4C burnable poison rods

Figure 2.2. One-Eight Core Layout (BOC Initial Conditions)

Table 2.1. Steady-State Calculation Results for Rod Worths

Case Index	Rod Position	Delayed Neutron Fraction, β (pcm)	Rod Worth (pcm / β)
EOC Centre	Assembly H8	521.10	349.3 / 0.670
EOC Periphery	Assembly N12	521.10	472.8 / 0.907
BOC Centre	Assembly H8	632.34	273.5 / 0.432
BOC Periphery	Assembly N12	632.34	548.5 / 0.867

Because of the REA start-up conditions corresponded to HZP with homogeneous thermal-hydraulic characteristics over the core, the RELAP thermal-hydraulics input deck was the same in all cases. An assembly-average representation of fuel and coolant parameters with 24 axial nodes was used to treat the core thermal-hydraulics. Besides, in each calculation a separate heat structure was chosen to represent the hottest fuel pin in the reactor core. The coolant thermal-hydraulic parameters for this heat structure corresponded to those for an assembly where the hottest pin was located.

The following features were investigated: core power and reactivity, fuel assembly powers, temperatures and enthalpies including their local values. Table 2.2 presents major core parameters of four REAs calculated by RELAP–BARS. The peak values of fuel temperature and enthalpy occur at the end of the transient (2.5 s). Total fuel enthalpy may be defined by adding the initial value of about 17 cal/g. Position of the hottest pins within a 15×15 PWR standard fuel assembly (FA) is given in Figure 2.3. Axial position of the hottest fuel pellet is given in terms of axial nodes (totally 24) from the bottom of the core. The core height is 357.12 cm, therefore, the node size is 14.88 cm. Thus, Node 22 is located between 312.5 cm and 327.4 cm from the core bottom. In the BOC cases the hottest pellet is located between Nodes 19 and 20, i.e. between 267.8 and 297.6 cm. The power peaking factors (total, F_q, radial, F_r, and axial, F_z) are given at 0.15-0.2 s (when they reach their maximum values) and at the end of the transient (2.5 s).

Figures 2.4 through 2.7 give assembly-average power distributions obtained in four REAs at time when the core power reaches its maximum and at the end of the transient (2.5 s). All distributions are normalized to an average value and, therefore, the maximum value shows the assembly-average radial peaking factor (at the end of the transient they coincide with those given in Table 2.2).

A comparison between the assembly-average and pin-by-pin radial peaking factors shows about 10%-difference in the cases with ejection of the central rod and more then 25%-difference in the cases with ejection of the peripheral rod. It is very important in regard to definition of the hottest fuel pin by indirect methods, such as a flux reconstruction, in assembly-by-assembly calculations. Since the peripheral fuel assemblies have, as a rule, higher intra-assembly power peaking factor, it is of interest to consider them from the point of view of intra-assembly power distribution. For instance, in Case EOC Periphery it was found that in the vicinity of the ejected rod (position N12) there were 5 hot fuel assemblies: N12 and two symmetrical N13 and M12. Their mean powers were within 5%-uncertainty. In spite of the fact that the last assembly had the peak power, the hottest fuel pin belonged to Assembly N13, diagonally adjacent to the core reflector. In turn, the intra-assembly peaking factor for this assembly was 1.26 whereas for the rest of the hot assemblies it was 1.11. As a result, 15%-underestimation in fuel enthalpy increase for the hottest fuel pin can occur only due to incorrect definition of its position.

Table 2.2. Core Parameters in REAs

Case Index $\rightarrow$	EOC Centre	EOC Periphery	BOC Centre	BOC Periphery
Ejected Rod Worth (pcm / β)	630.9 / 1.2107	631.0 / 1.2109	765.7 / 1.2109	765.7 / 1.2108
Peak Power (GW / % Nominal)	11.05 / 398.6	4.39 / 158.2	37.49 / 1352.5	13.07 / 471.4
Time of Peak Power (ms)	335.9	298.2	254.2	243.0
Power Pulse Width (ms)	61.9	64.5	39.8	41.4
Core-Average Fuel Temperature (K)	590.2	568.8	664.3	594.9
Maximum FA Temperature (K)	812.0	785.6	898.9	898.0
Maximum Fuel Pin Temperature (K)	835.3	851.6	935.9	996.1
Maximum FA Enthalpy Increase (cal/g)	18.88	16.87	25.52	25.45
Max. Pin Enthalpy Increase (cal/g)	20.65	21.90	28.37	33.04
Position of the Hottest Assembly	H9	M12	H9	N13
Position of the Hottest Fuel Pellet	H9 Node 22	N13 Node 22	H9 Nodes 19, 20	N13 Nodes 19, 20
Pin-by-Pin Total F_q (max / at 2.5 s)	8.04 / 6.51	20.1 / 16.2	4.11 / 3.09	12.9 / 9.52
Assembly-Average F_q' (max / at 2.5 s)	7.42 / 6.03	16.0 / 13.0	3.71 / 2.79	10.2 / 7.51
Pin-by-Pin Radial F_r (max / at 2.5 s)	2.91 / 2.66	7.42 / 6.61	2.73 / 2.48	8.76 / 7.40
Assembly-Average F_r' (max / at 2.5 s)	2.68 / 2.46	5.93 / 5.32	2.46 / 2.24	6.91 / 5.83
Average Axial F_z (max / at 2.5 s)	2.76 / 2.45	2.71 / 2.44	1.50 / 1.25	1.47 / 1.29

					R				R					
			R	2							R			
			2,4											
1		R			R				R			R		
							3							
						3	C	3						
							3							
1		R			R				R			R		
			2											
			R								R			
					R				R					

$\boxed{R}$ - control rod guide tube

$\boxed{C}$ - instrumentation tube

1 - EOC Centre

2 - EOC Periphery

3 - BOC Centre

4 - BOC Periphery

Figure 2.3. Position of the Hottest Pins in Fuel Assembly during REAs

	8	9	10	11	12	13	14	15
H	2.070 1.926	2.631 2.463	1.857 1.756	1.710 1.646	0.649 0.641	0.757 0.774	0.336 0.352	0.236 0.249
K		1.950 1.830	1.982 1.884	1.338 1.296	1.222 1.218	0.561 0.576	0.835 0.876	0.334 0.353
L			0.874 0.841	1.321 1.301	1.091 1.103	1.215 1.257	1.002 1.054	0.351 0.372
M				0.634 0.638	1.128 1.159	0.938 0.976	0.699 0.736	
N					0.617 0.642	0.986 1.038	0.457 0.483	
O			$t = t_{max}$ → $t = 2.5$ s →			0.564 0.597		

2.631 2.463	- FA with peak power and the hottest pin

Figure 2.4. Assembly-Average Power Distributions (Case EOC Centre)

		4	5	6	7	8	9	10	11	12	13	14	15
				0.068	0.068	0.056	0.091	0.101					
				0.096	0.094	0.075	0.119	0.131					
		0.083	0.132	0.197	0.174	0.082	0.234	0.300	0.226	0.162			
		0.119	0.186	0.274	0.238	0.109	0.303	0.385	0.285	0.201			
	0.102	0.182	0.182	0.249	0.126	0.198	0.167	0.389	0.324	0.378	0.243		
	0.146	0.258	0.253	0.339	0.167	0.253	0.210	0.486	0.401	0.461	0.291		
		0.119	0.232	0.244	0.305	0.186	0.394	0.382	0.436	0.277	0.491	0.243	
		0.165	0.314	0.320	0.386	0.228	0.477	0.461	0.522	0.325	0.571	0.280	
			0.142	0.326	0.367	0.527	0.466	0.525	0.305	0.622	0.551	0.436	
			0.186	0.411	0.447	0.625	0.544	0.606	0.345	0.700	0.619	0.489	
				0.237	0.582	0.608	0.771	0.431	0.804	0.724	0.845	0.741	0.275
				0.287	0.685	0.698	0.864	0.471	0.867	0.783	0.921	0.808	0.298
					0.590	0.870	0.874	1.215	1.012	1.035	0.522	0.798	0.334
					0.675	0.966	0.937	1.271	1.047	1.071	0.541	0.835	0.348
H						0.544	1.418	1.450	1.772	0.853	1.181	0.570	0.408
						0.580	1.465	1.464	1.759	0.833	1.149	0.554	0.398
K							1.454	2.152	2.150	2.610	1.404	2.202	0.863
							1.461	2.111	2.059	2.458	1.314	2.067	0.813
L								1.544	3.700	3.583	4.108	3.229	1.069
								1.474	3.465	3.310	3.789	2.998	0.998
M									4.042	5.792	4.221	2.787	
									3.726	5.316	3.856	2.564	
N										5.506	5.734	2.257	
										5.011	5.241	2.067	
O											3.343		
											3.050		

$t = t_{max}$ →
$t =$ 2.5 s →

5.792
5.316

- FA with peak power

5.734
5.241

- FA with the hottest pin

Figure 2.5. Assembly-Average Power Distributions (Case EOC Periphery)

	8	9	10	11	12	13	14	15
H	1.847 1.712	2.409 2.237	1.969 1.844	1.694 1.620	0.713 0.709	0.736 0.758	0.330 0.349	0.169 0.180
K		1.979 1.840	1.942 1.831	1.431 1.377	1.180 1.178	0.617 0.637	0.857 0.906	0.258 0.275
L			0.983 0.943	1.301 1.278	1.072 1.085	1.141 1.184	1.046 1.105	0.280 0.298
M				0.717 0.726	1.135 1.170	0.954 0.996	0.630 0.666	
N					0.744 0.780	1.138 1.201	0.406 0.431	
O			$t = t_{max}$ → $t = 2.5$ s →			0.572 0.608		

2.409 2.237	- FA with peak power and the hottest pin

Figure 2.6. Assembly-Average Power Distributions (Case BOC Centre)

	4	5	6	7	8	9	10	11	12	13	14	15
			0.053 0.080	0.051 0.076	0.039 0.056	0.068 0.095	0.078 0.108					
	0.072 0.110	0.116 0.175	0.200 0.300	0.174 0.257	0.079 0.112	0.234 0.323	0.303 0.415	0.196 0.264	0.139 0.183			
0.100 0.154	0.203 0.311	0.180 0.269	0.230 0.336	0.137 0.195	0.190 0.260	0.180 0.241	0.355 0.472	0.321 0.420	0.417 0.540	0.230 0.293		
	0.138 0.208	0.229 0.333	0.239 0.335	0.297 0.400	0.205 0.268	0.379 0.485	0.370 0.472	0.427 0.540	0.313 0.390	0.519 0.640	0.197 0.240	
		0.160 0.224	0.326 0.436	0.402 0.517	0.535 0.668	0.506 0.620	0.517 0.626	0.333 0.397	0.586 0.693	0.519 0.612	0.366 0.429	
			0.274 0.351	0.594 0.735	0.673 0.810	0.782 0.914	0.490 0.555	0.775 0.865	0.682 0.765	0.754 0.853	0.730 0.825	0.204 0.230
				0.637 0.765	0.861 0.997	0.938 1.040	1.216 1.307	1.073 1.137	0.976 1.037	0.552 0.588	0.772 0.831	0.240 0.258
H					0.570 0.628	1.398 1.477	1.574 1.617	1.736 1.746	0.911 0.900	1.112 1.089	0.543 0.530	0.284 0.278
K						1.551 1.579	2.132 2.104	2.241 2.143	2.433 2.271	1.505 1.392	2.227 2.062	0.661 0.616
L							1.709 1.623	3.530 3.253	3.453 3.119	3.810 3.429	3.328 3.022	0.847 0.778
M								4.258 3.815	5.795 5.120	4.360 3.844	2.528 2.256	
N									6.293 5.504	6.669 5.833	2.052 1.809	
O										3.408 2.981		

$t = t_{max}$ →
$t = 2.5$ s →

6.669
5.833
- FA with peak power and the hottest pin

Figure 2.7. Assembly-Average Power Distributions (Case BOC Periphery)

For this study with relatively simple scenario of the transient starting from HZP, it was not so difficult to define the hottest pins in advance. It is clear, that as can be seen in Figures 2.1 and 2.2, in the cases with ejection of the central rod the hottest pins have to be located in Assembly H9 (adjacent to Assembly H8) with relatively low fuel burnup. Analogously, in cases with ejection of the peripheral rod the hottest pins are to be located somewhere in Assemblies M12, N13 or even N12 with the highest powers. But in many other cases with rather complicated spatial power distribution history, the flux reconstruction procedure may encounter serious difficulties. Another problem is use of this procedure for the peripheral assemblies adjacent to the core reflector where the flux reconstruction method may lead to significant uncertainty in pin powers.

Core-average axial power distributions are given in Figure 2.8 for two cases with ejection of the central rod at EOC and BOC at two time moments: 0.2 s and the end of the transient. It can be seen from Figures 2.4 through 2.8 and the data presented in Table 2.2, that the power peaking factor decreases due to the core heat-up during the transient: by 20% at EOC and by 25% at BOC.

Figures 2.9 through 2.16 presents the following parameters as a function of time of the transients: the core power, reactivity, and peaking factors for the first second, and the fuel temperature and fuel enthalpy increase for the hottest fuel pins. As can be seen in Figures 2.9-2.12, the power excursion starts at about 0.2 s. The power reaches a peak value at 0.24-0.34 s, then, due to negative reactivity feedback the power excursion is terminated.

The power pulse width is 62-65 ms at EOC and about 40 ms at BOC, thus, the power pulse (with the right boundary of 10% of a peak power) lies within 0.2-0.4 s at EOC and within 0.2-0.3 s at BOC. Reactivity reaches its maximum at 0.13-0.15 s due to withdrawal of the ejected rod and continues to be constant during about 0.10-0.15 s. Then reactivity begins to drop as a result of the negative reactivity feedback due to fuel heat-up and, later, due to coolant heat-up. At the time of the core peak power, reactivity is equal to approximately 1β. The behavior of the total power peaking factor, F_q, is rather similar: firstly it increases due to the rod ejection, then there is a “plateau” area with further decrease due to the core heat-up.

Figures 2.13 through 2.16 indicate that about 80% of the fuel enthalpy increase is produced during first 0.5-0.6 s after the rod ejection. It should be noted also that in the cases with ejection of the peripheral control rod, 50% of the core energy is produced only in several fuel assemblies: 17 at BOC and 23 at EOC, i.e. about 10-13% of the total number of fuel assemblies in the core (177).

Now consider an influence of spatial effects on the REA parameters. As it can be seen in Table 2.2 and Figures 2.9-2.16, noticeable differences in the power peak, fuel temperature and enthalpy increase occur. In the cases with ejection of the peripheral rod the peak power is lower than that in the cases with ejection of the central rod: by 2.5 times at EOC and by 2.9 times at BOC. On the other hand, practically the same, but inverse relationship occurs for the power peaking factor. The total core energy deposition can be characterized by a core-average fuel temperature increase. This parameter shows a similar tendency: corresponding ratio for the rod ejection cases is 2.2 at EOC and 2.6 at BOC. Consequently, it is worth to conclude that there is an evident correlation between the peak power, reactor energy deposition and the power peaking factor, F_q : the higher the F_q value, the lower the peak power and energy deposition in the core. However, it is clear, that a REA with the highest magnitude of F_q is more severe from the point of view of the local fuel enthalpy increase. Thus, in fact, the effect of the power peaking factor is revealed in two opposite directions, namely, a higher value of the peaking factor tends to decrease the total energy deposition in the core and, on the other hand, to increase the local fuel enthalpy.

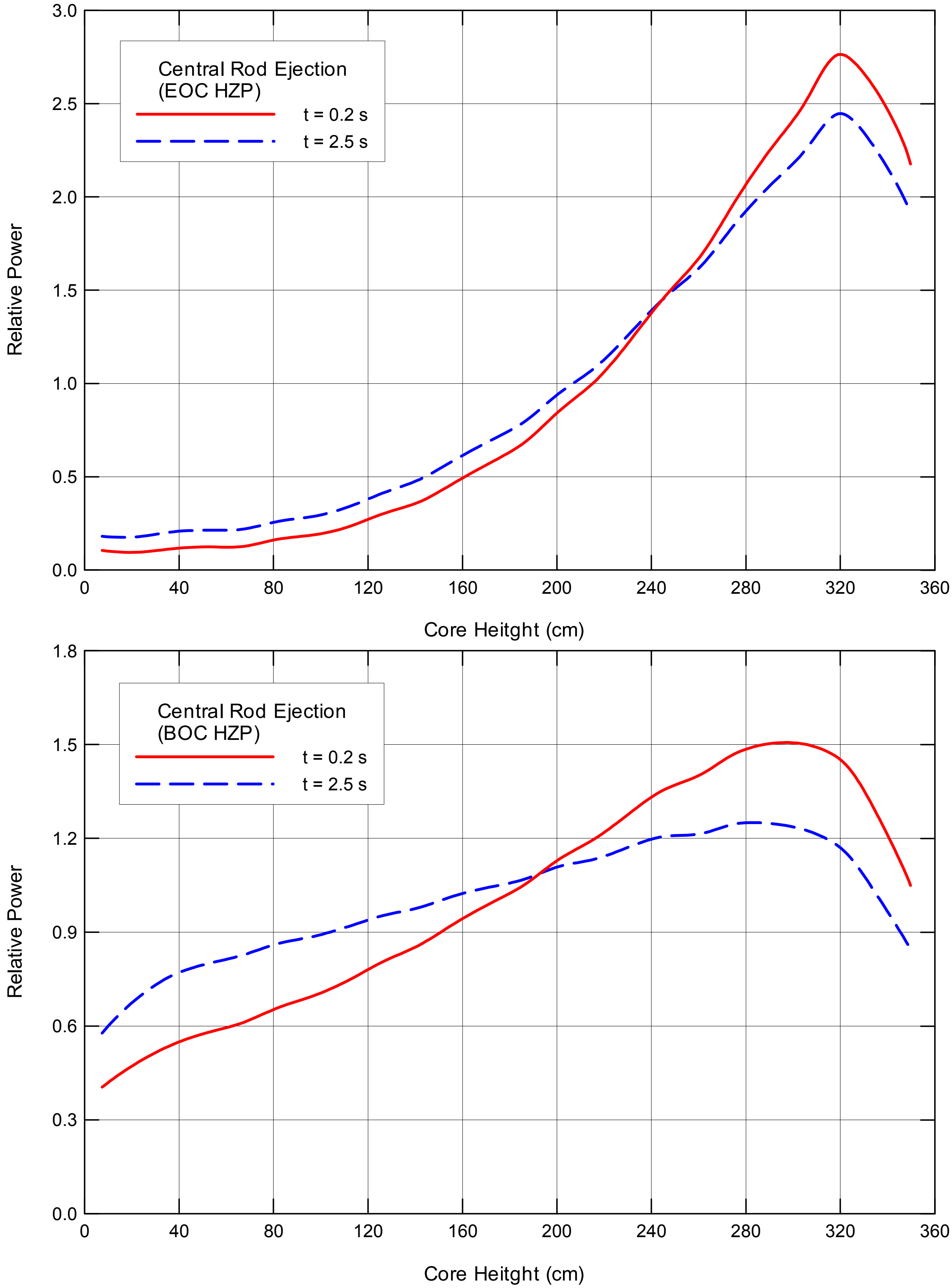

Figure 2.8. Average Axial Power Distribution (Cases EOC and BOC Centre)

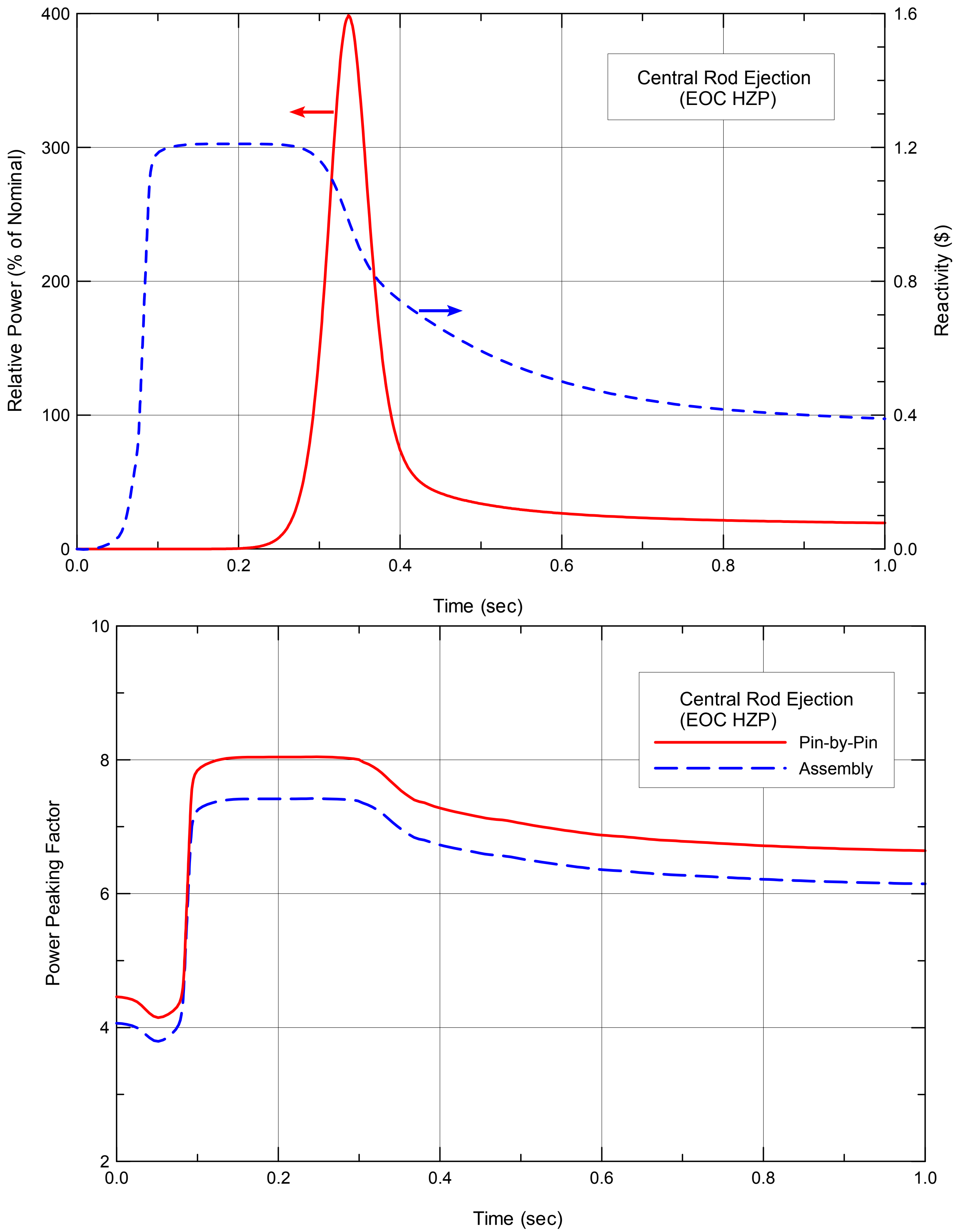

Figure 2.9. Power, Reactivity and Peaking Factors vs. Time (Case EOC Centre)

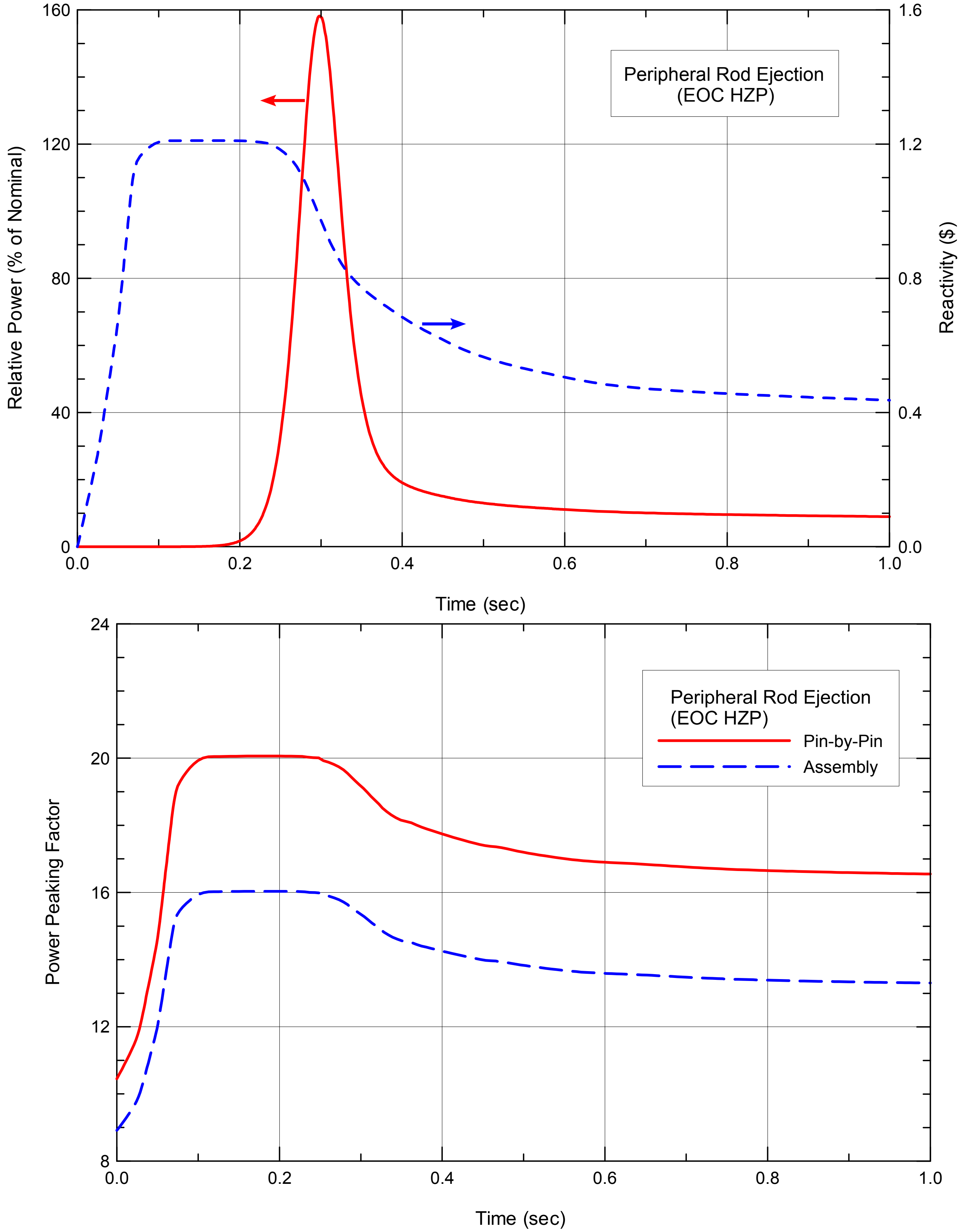

Figure 2.10. Power, Reactivity and Peaking Factors vs. Time (Case EOC Periphery)

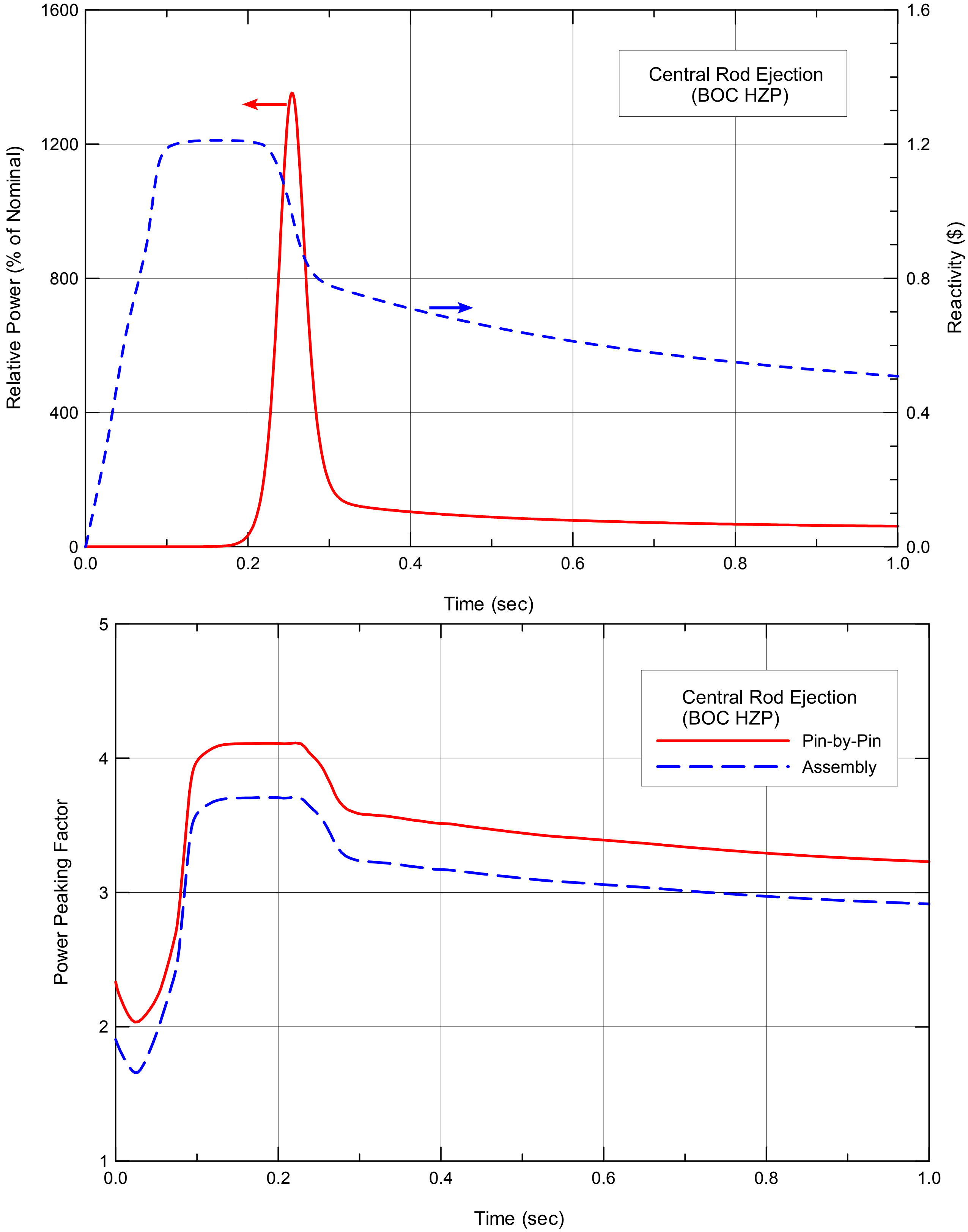

Figure 2.11. Power, Reactivity and Peaking Factors vs. Time (Case BOC Centre)

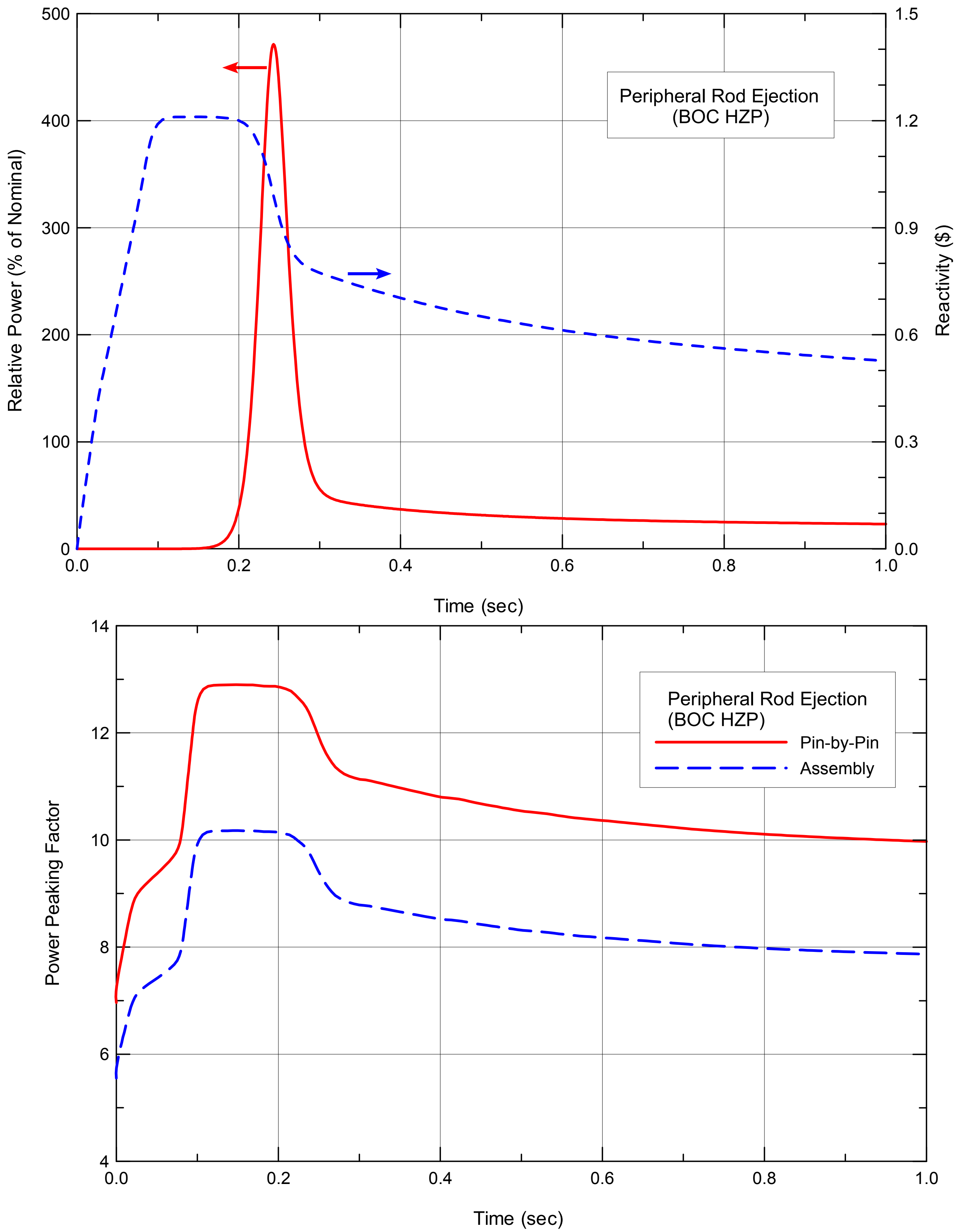

Figure 2.12. Power, Reactivity and Peaking Factors vs. Time (Case BOC Periphery)

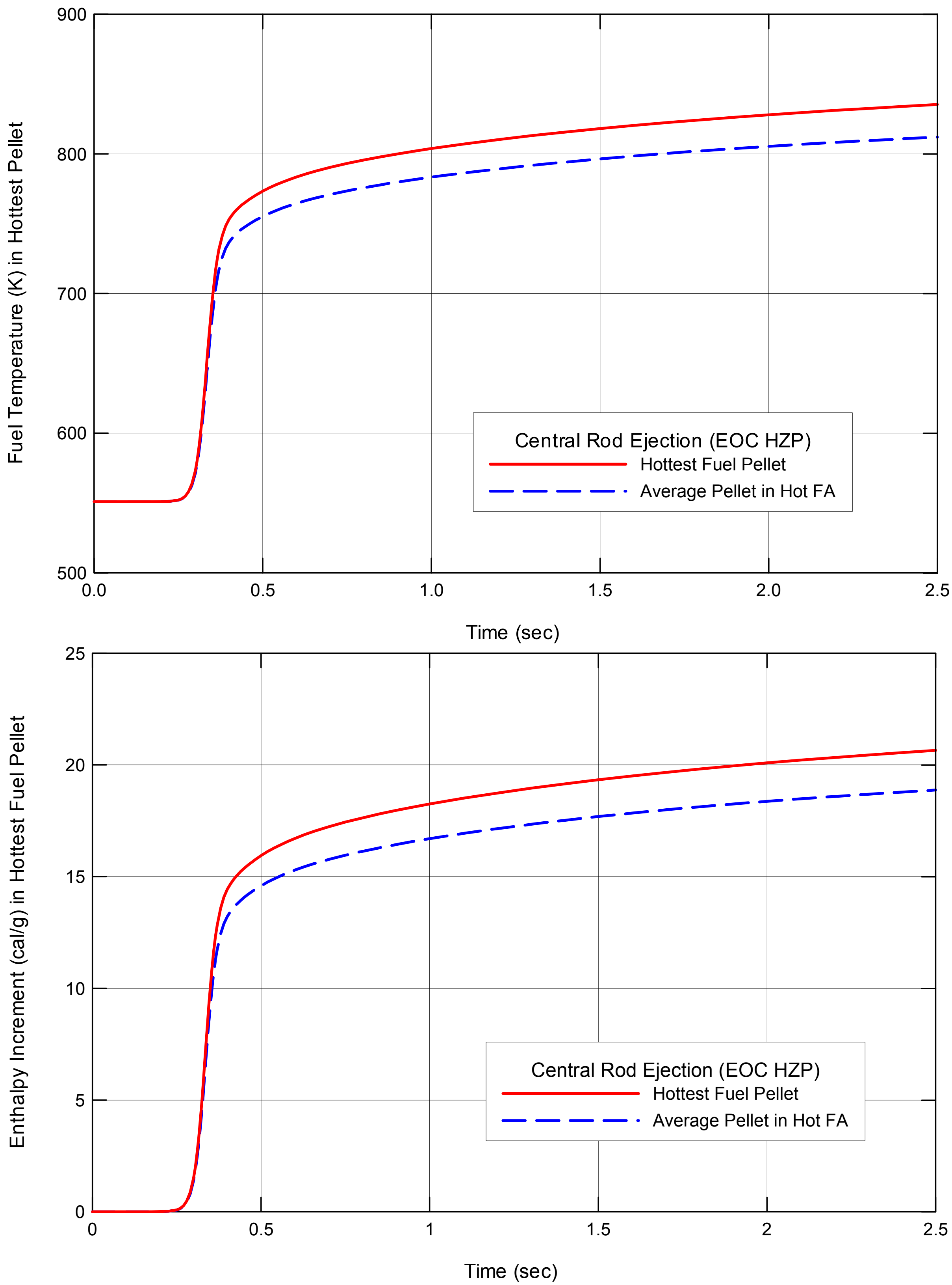

Figure 2.13. Fuel Temperature and Enthalpy in Hot Pins vs. Time (Case EOC Centre)

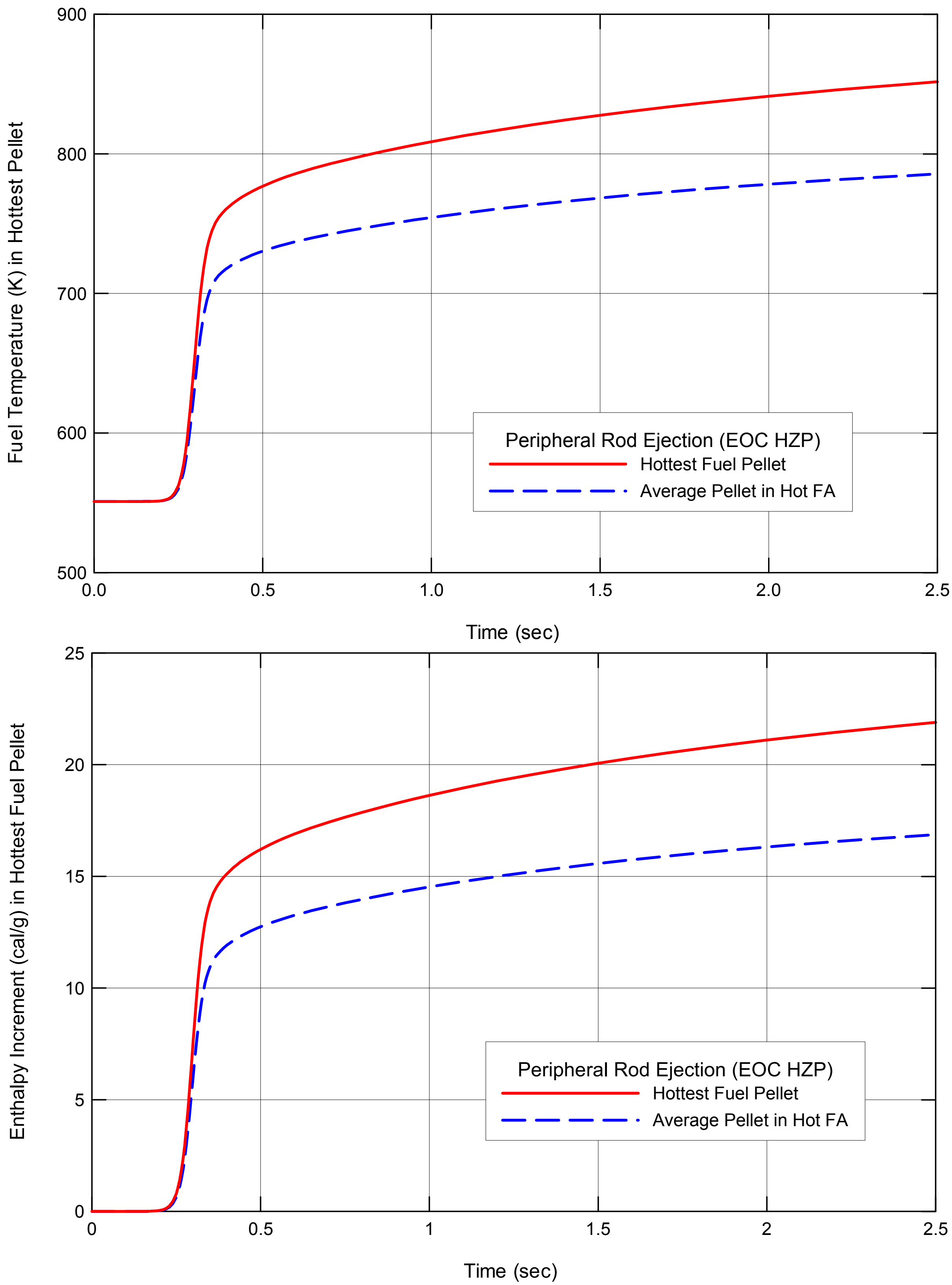

Figure 2.14. Fuel Temperature and Enthalpy in Hot Pins vs. Time (Case EOC Periphery)

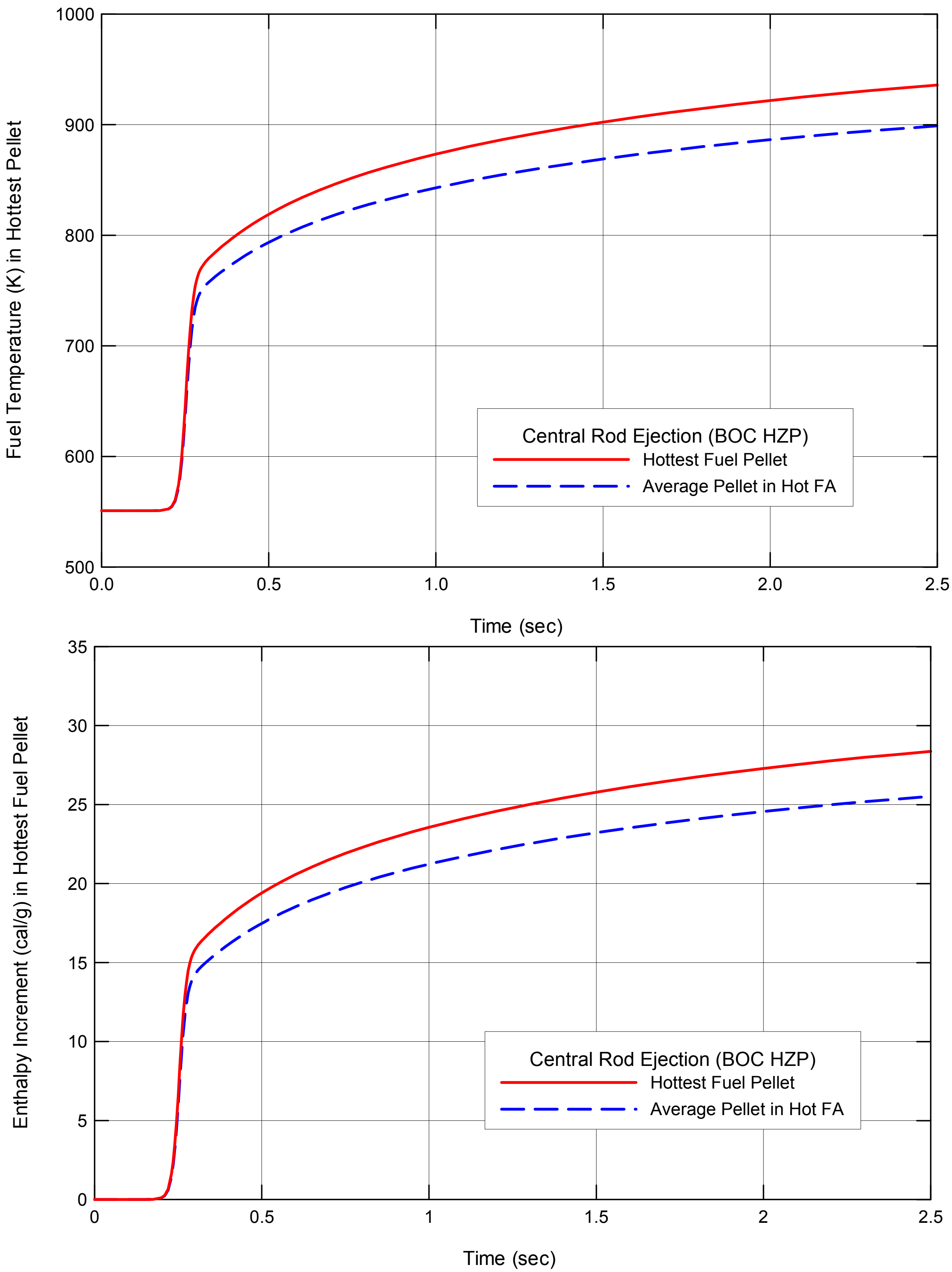

Figure 2.15. Fuel Temperature and Enthalpy in Hot Pins vs. Time (Case BOC Centre)

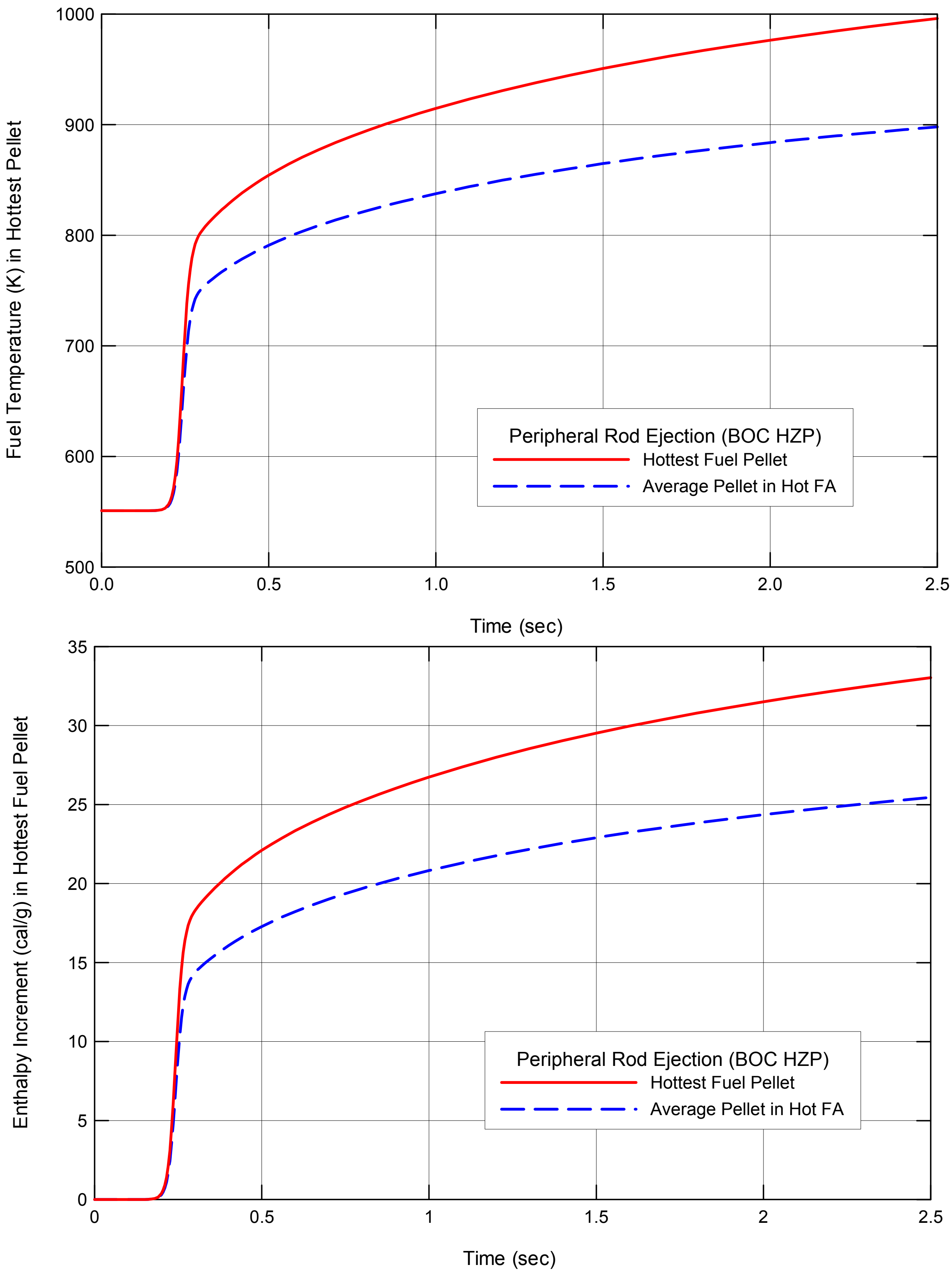

Figure 2.16. Fuel Temperature and Enthalpy in Hot Pins vs. Time (Case BOC Periphery)

As can be seen in Table 2.2 both cases with ejection of the peripheral rod show lower core-average fuel temperature compared with the cases with ejection of the central rod: 569 K at EOC and 595 K at BOC against 590 K and 664 K, respectively. Practically the same picture is observed for the peak assembly-average temperatures at EOC: 786 K against 812 K. But in the BOC cases they are very close: 899 K and 898 K. Consequently, the similar situation was found for the maximum assembly-average enthalpy increase: 16.9 cal/g against 18.9 cal/g at EOC, and about 25.5 cal/g in both BOC cases.

Therefore, from the point of view of assembly-by-assembly representation, both cases with ejection of the central control rod result in higher values of the assembly-average enthalpy increase compared with ejection of the peripheral rod. The next step is a definition of the hottest fuel pin. Consider the EOC cases. If this procedure is performed for the hottest fuel assembly, then we need the intra-assembly peaking factors for Assembly H9 (Case EOC Centre) and Assembly M12 (Case EOC Periphery). For both assemblies these factors were about 1.1. Thus, it can be expected the following values for the maximum pin enthalpy increase: 18.6 and 20.7 cal/g for ejection of the peripheral and central rod, respectively. As can be compared with the data presented in Table 2.2, such an approach leads to about 18% underestimation in the maximum pin enthalpy for Case EOC Periphery.

In the BOC cases the assembly-average parameters (the maximum fuel temperature and enthalpy) were found as approximately the same (899 K and 25.5 cal/g, respectively). The intra-assembly peaking factor was about 1.1 for Assembly H9 (Case BOC Centre) and about 1.27 for Assembly N13 (Case BOC Periphery). Thus, the maximum fuel pin enthalpy increase is estimated as 32.3 and 28.1 cal/g for ejection of the peripheral and central rod, respectively. The last values are close to those obtained from the pin-by-pin calculations (see Table 2.2).

Thus, the pin-by-pin calculations show that the peak fuel pin enthalpy increase is higher in both cases with ejection of the peripheral rod: 21.9 cal/g at EOC and 33.0 cal/g at BOC against 20.7 cal/g and 28.4 cal/g, respectively.

To investigate the influence of the power peaking factor on major REA parameters it is of interest to consider a simple approximation as described in the next section. This approach based on a Nordheim-Fuchs model (Ref. 6), which is well-known and widely used for analytical estimations of different neutronic parameters in pulsed reactors.

2.2 Nordheim-Fuchs Model

This model is valid when the rod worth is greater than the value of the delayed neutron fraction, β. Next assumption is that the reactivity change due to feedback is proportional to the energy deposition. We will consider also an adiabatic approximation when there is no heat transfer to the coolant. Then using the point kinetics equations, the reactivity is:

$$\rho(t) = \rho_o - \gamma Q(t) \qquad (1)$$

where ρ_o is the reactivity worth of the ejected rod, γ is the feedback parameter, and $Q(t)$ is the energy deposition. As it can be shown (Ref. 6), the peak power, P_{max}, and the total energy deposition, Q_{tot}, are:

$$P_{max} = (\rho_o - \beta)^2 / (2\Lambda\gamma) \qquad (2)$$

and

$$Q_{tot} = 2\,(\rho_o - \beta)/\gamma \tag{3}$$

where Λ is the prompt neutron lifetime. According to Eq. (1) the feedback parameter is:

$$\gamma = -\delta\rho / \delta Q \tag{4}$$

where δQ is the energy deposition increase and $\delta\rho$ is the corresponding change in the reactivity. The adiabatic assumption means that the only feedback is the Doppler effect, thus, δQ and $\delta\rho$ can then be expressed in terms of the change in fuel temperature, ΔT:

$$\delta Q = \int_V C_p\, \Delta T\, dV \tag{5}$$

and

$$\delta\rho = < \varphi^+, \alpha_D\, \Delta T\, \psi > \tag{6}$$

where C_p is the fuel heat capacity, V is the fuel volume in the core, φ^+ is the adjoint flux solution for the initial steady state, α_D is the fuel temperature (Doppler) reactivity coefficient, and ψ is the neutron flux with the following normalization condition:

$$< \varphi^+, \psi > = 1 \tag{7}$$

where the inner product represents integral over energy and the core volume. For further analysis it is worth to simplify both Eq. (5) and Eq. (6) if the fuel heat capacity and the Doppler coefficient are assumed to be constant. Such an approximation yields:

$$\delta Q = C_p\, V\, \Delta T_{avr} \tag{8}$$

and

$$\delta\rho = \alpha_D < \varphi^+, \Delta T\, \psi > \tag{9}$$

where ΔT_{avr} is the average change in fuel temperature over the core. In this case Eq. (4) can be expressed as:

$$\gamma = \gamma_o < \varphi^+, \Delta T\, \psi > / \Delta T_{avr} \tag{10}$$

where

$$\gamma_o = -\alpha_D / (C_p\, V)\ . \tag{11}$$

It can be seen that $\gamma = \gamma_o$ under the assumption of constant ΔT, i.e. $\Delta T = \Delta T_{avr}$. In other words it means that γ_o represents the feedback parameter in case when fuel temperature changes by the same value in each fuel pellet over the core. This is possible when power distribution is uniform in both radial and axial directions. It is obvious, that γ_o is the lower limit of the feedback parameter (α_D is always negative) and, thus, provides the maximum values of the peak power, P_{max}, and the total energy deposition, Q_{tot}, as seen from Eq. (2) and Eq. (3). To estimate the upper limit of γ, it is necessary to keep in mind that generally ΔT and weight functions φ^+ and ψ in Eq. (10) have quite different spatial distributions. Nevertheless, taking into account Eq. (7) the upper limit of the feedback parameter, γ_{max}, can be estimated as follows:

$$\gamma_{max} = \gamma_o \, \Delta T_{max} / \Delta T_{avr} \qquad (12)$$

where ΔT_{max} is the maximum change in fuel temperature over the core. $\Delta T_{max}/\Delta T_{avr}$ is the peaking factor for the change in fuel temperature. Under the adiabatic assumption, its value practically coincides with the power peaking factor, F_q. Then, the upper limit of γ is:

$$\gamma_{max} = \gamma_o \, F_q \ . \qquad (13)$$

Thus, both limits are proportional to the power peaking factor (taking into account that F_q is equal to 1 for the lower limit). Therefore, one can expect also that γ may be approximated as a linear function of F_q. In the present study, based on the RELAP-BARS calculations this evaluation was done.

Figure 2.17 shows the relative feedback parameter, γ/γ_o, as a function of the pin-by-pin and assembly-average power peaking factors, F_q and F_q', respectively. As shown in the figure, both dependencies, $f(F_q)$ and $f(F_q')$, are approximately linear functions. More precise approximations for γ were found as follows:

$$\gamma \approx \gamma_o \, (0.38 \, F_q + 0.24) \qquad (14)$$

and

$$\gamma' \approx \gamma_o \, (0.50 \, F_q' - 0.09) \ . \qquad (15)$$

For the present analysis we can estimate the values of the feedback parameter, γ, during considered transients. At HZP conditions (T = 551 K) the value of the fuel heat capacity, C_p, is about 3.0 MJ/(m^3K). The fuel volume in the TMI-1 core is 9.2 m^3. The fuel temperature (Doppler) coefficient is about 2.8 pcm/K. Therefore, according to Eq. (11):

$$\gamma_o \approx 1.0 \times 10^{-6} \ \ MJ^{-1} \ . \qquad (16)$$

This result was also confirmed by the RELAP–BARS calculation of Case EOC Centre under an assumption of the uniform heat-up over the core volume (i.e. when $\Delta T = \Delta T_{avr}$). Besides aforementioned peak power and total energy deposition, the power pulse width at the pulse half, $\Delta t_{1/2}$, can be estimated (within the Nordheim-Fuchs model) as follows:

$$\Delta t_{1/2} = 3.53 \, \Lambda / (\rho_o - \beta) \ . \qquad (17)$$

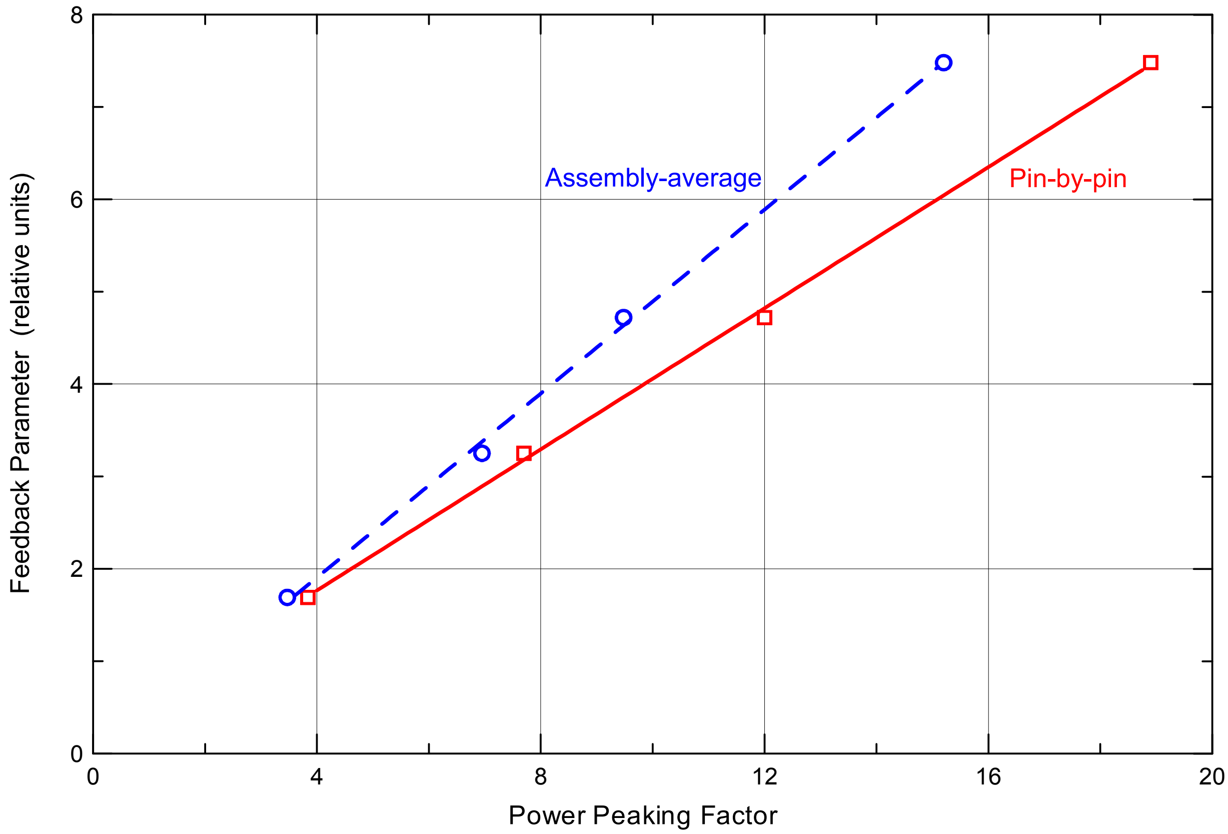

Figure 2.17. Feedback Parameter vs. Power Peaking Factor

The Nordheim-Fuchs model does not take into account the effects of delayed neutrons. For this reason an applicability of this approach is restricted by the power pulse area. For the present study it means that this model is valid only to 0.4 s at EOC and to 0.3 s at BOC. Instead of the total energy deposition, Q_{tot}, as defined by Eq. (3), we will use the energy deposition at the power peak time, Q_o, which equals to $Q_{tot} / 2$. Table 2.3 presents some of the neutronic parameters of interest obtained from the RELAP–BARS calculations of the transients. The prompt neutron lifetime, Λ, feedback parameter, γ, and peaking factors, F_q and F_q', were averaged over those limits. The core energy deposition, Q_o, was defined as integral of the total core power up to the time of the power peak.

Table 2.3. Some Neutronic Parameters of REAs

Parameter	EOC Centre	EOC Periphery	BOC Centre	BOC Periphery
Core Energy Deposition, Q_o (GJ)	0.366	0.149	0.818	0.292
Prompt Neutron Lifetime, Λ (s)	1.86×10^{-5}	1.87×10^{-5}	1.46×10^{-5}	1.49×10^{-5}
Feedback Parameter, γ (MJ^{-1})	3.25×10^{-6}	7.48×10^{-6}	1.69×10^{-6}	4.72×10^{-6}
Pin-by-Pin Total Peaking Factor, F_q	7.70	18.9	3.84	12.0
Assembly-average Peaking Factor, F_q'	6.95	15.2	3.47	9.48

Using the data presented in Table 2.3 and the ejected rod worth (see Table 2.2) it is easy to evaluate the following parameters: P_{max}, Q_o, γ and $\Delta t_{1/2}$ by Eq. (2), (3), and (15)–(17). Table 2.4 contains these evaluated parameters.

A comparison between the data presented in Table 2.4 with the calculated results (see Tables 2.2 and 2.3) shows that the peak power, P_{max}, and core energy deposition, Q_o, are underestimated by 3–10%. Practically the same uncertainties are found for the power pulse width, $\Delta t_{1/2}$. Both feedback parameters are estimated within 5% uncertainty. (It should be noted, that the approximations defined by Eq. (14) and Eq.(15) may differ for REAs with other neutronic parameters.)

Table 2.4. Evaluated Neutronic Parameters of REAs

Parameter	EOC Centre	EOC Periphery	BOC Centre	BOC Periphery
Peak Power (GW / % Nominal)	9.97 / 360	4.32 / 156	36.0 / 1300	12.6 / 456
Core Energy Deposition, Q_o (GJ)	0.338	0.147	0.789	0.282
Feedback Parameter, γ (MJ^{-1})	3.17×10^{-6}	7.42×10^{-6}	1.70×10^{-6}	4.80×10^{-6}
Feedback Parameter, γ' (MJ^{-1})	3.38×10^{-6}	7.51×10^{-6}	1.65×10^{-6}	4.65×10^{-6}
Power Pulse Width, $\Delta t_{1/2}$ (ms)	59.8	60.1	38.6	39.5

Thus, these results confirm an assumption about strict correlation between the peak power, core energy deposition and as a result, fuel temperature (or enthalpy) increase, and the power peaking factor. Presented simplified estimations allow to conclude the following fact: the feedback parameter, γ, is approximately proportional to the power peaking factor. In its turn, both the peak power and energy deposition are inversely proportional to γ and, as a result, to the power peaking factor.

Therefore, it may be concluded that if the adiabatic assumption were valid during a REA, it would be expected that the peak fuel enthalpy increase practically does not depend on spatial effects. In other words, in the transients with quite different power distributions in the radial and axial directions, but with the same neutronic parameters, ρ_o and β, the results for the peak fuel enthalpy increase are to be obtained as very similar.

Of course, a REA may be considered as an adiabatic process in terms of energy deposition only within a narrow time interval limited by the power pulse area when a very fast rise and decrease of power takes place. When power decreases to about 10% of its peak value, effects of delayed neutron become distinct. After the power pulse, the energy deposition process is rather mild. During the present study with 1.21β REAs it was found the following. Just after the termination of the power pulse (at 0.4 s at EOC or 0.3 s at BOC) about 3-4% of fuel energy release is transmitted to the coolant; this value becomes about 20% at 1 s. Besides, the prompt fraction of energy deposition (within the limits of the power pulse when the adiabatic assumption is valid) gives only about 30-40% of the total energy deposition at the end of the transient. On this evidence, it is clear that the above reasoning should be considered as very approximate. It should be also taken into account that the feedback parameter, γ, changes by several times during the transient as calculated by RELAP-BARS. As it can be seen in Figures 2.13 and 2.14 for the EOC cases, the difference between the assembly-average fuel enthalpy increase reaches 10% already at 0.4 s. From the other hand, as shown in Figures 2.15 and 2.16, for the BOC cases this difference is very small. Nevertheless, above mentioned simplified approach may be very useful to estimate some important parameters of a REA.

2.3 Results of Steady-State Calculations

Recently an intercomparison of PWR REA calculations performed by different codes has been carried out (Ref. 5). In the framework of that study a number of steady-state calculations were done using the following neutronic codes: BARS (Ref. 1), PARCS (Ref. 7) and CRONOS2 (Ref. 8), developed in the Russian Federation, the United States, and France, respectively. PARCS and CRONOS2 are assembly-by-assembly nodal diffusion codes. During that study they used the same two-group cross-sections generated with the CASMO-3 code. BARS used four-group lambda-matrices generated with the TRIFON code. The reactor model was the same as defined in Section 2 for Case EOC Centre (see also Figure 2.1).

Among those steady-state calculations there were calculations of each control rod in Bank 7 at HZP conditions. Table 2.5 presents the results of the steady-state calculations of the rod worths. Last column indicates average deviations of the BARS data from the PARCS and CRONOS2 results. Comparison of the rod worths shows that the differences between the PARCS and CRONOS2 results do not exceed 3%. The BARS result is slightly higher for Rod H8 (by 1%); the deviation for Rod H12 is 8%. The most deviation was found for Rod N12 (about 35%).

The same steady-state calculations but at BOC HZP conditions (see Figure 2.2) have been performed by the PARCS code (Ref. 9). Table 2.6 presents those results in comparison with the BARS data. As can be seen in Table 4.2, the most deviations occur for Rod H8 (18%) and Rod N12 (15%). The deviation for Rod H12 (9%) is practically the same as was found for EOC HZP case.

From a comparison of the data presented in Tables 2.5 and 2.6, the following observations can be obtained. The BARS results indicate that the heaviest rod (Rod N12) has a similar worth in terms of delayed neutron fraction, β, (about 0.9β) in both cases (at BOC its worth is 16% higher in absolute units). The PARCS results show that at BOC conditions the worth of Rod N12 is higher by 14% in absolute units and by 39% in terms of β. Nevertheless, 0.91β worth seems to be the highest one. For this reason to reach a prompt critical (i.e. a rod worth of more than 1β) in reality it is necessary to change the initial control rod arrangement in the core. If Rod M11 of Bank 5 is assumed to be stuck-out at the upper position (i.e. out of the core), the worth of Rod N12 can be significantly increased. As the BARS steady-state calculations show, the worth of Rod N12 is as follows:

- 907 pcm or 1.74 β at EOC HZP conditions;
- 954 pcm or 1.51 β at BOC HZP conditions.

The situation when a single control rod of any regulating bank is found as stuck-out at the upper or intermediate position, is possible as a result of any control system malfunction during a rector trip. Then if a reactor reaches a critical level at HZP, ejection of a control rod neighboring with a stuck rod may lead to a prompt critical.

In conclusion it should be noted that 35% uncertainty in the rod worth as was found during the above mentioned intercomparison between the PARCS and BARS steady-state results (see Table 2.5), may lead to a significant uncertainty in consequences of a REA, especially if the ejected rod worth is above 1β. For instance, in a 1.2β REA a 35% uncertainty in the ejected rod worth may results in about 300% uncertainty in the core energy deposition and, consequently, in the peak fuel enthalpy increase, as it can be seen from Eq. (3) presented in the previous section.

Table 2.5. Steady-State Calculational Results for EOC HZP Case

Parameter	BARS	PARCS	CRONOS2	Deviation
Worth of Rod H8 (pcm/β)	349 / 0.670	347 / 0.666	345 / 0.662	3 / 0.006
Worth of Rod H12 (pcm/β)	204 / 0.391	188 / 0.361	188 / 0.361	16 / 0.030
Worth of Rod N12 (pcm/β)	473 / 0.907	344 / 0.660	353 / 0.677	125 / 0.240

Table 2.6. Steady-State Calculational Results for BOC HZP Case

Parameter	BARS	PARCS	Deviation
Worth of Rod H8 (pcm/β)	273 / 0.432	230 / 0.363	43 / 0.069
Worth of Rod H12 (pcm/β)	164 / 0.259	150 / 0.237	14 / 0.022
Worth of Rod N12 (pcm/β)	548 / 0.867	477 / 0.754	71 / 0.113

3 UNCERTAINTY ANALYSIS

3.1 Methodology

The methodology of the uncertainty analysis is close to that developed in BNL. It is based on a sensitivity study to global quantities that are explicitly used in point kinetics equations or can be taken into account implicitly in point kinetics through thermal-hydraulic feedback. The approach does not require validity for the adiabatic assumption and is based on the non-adiabatic thermal-hydraulic model realized in the RELAP5/MOD3.2 code (Ref. 3).

Assuming that a safety parameter (y) is a function of a number of above quantities (x) and the random error in each quantity is normally distributed, the square of the uncertainty in the parameter y can be written:

$$(\delta y/y)^2 = \Sigma(S_x)^2(\delta x/x)^2 \qquad (18)$$

where $\delta x/x$ is the uncertainty in the quantity x, S_x is the sensitivity of the parameter y to the quantity x, and the summation is over all quantities of interest.

It was studied the uncertainty in the following safety parameters (y):

- peak local fuel enthalpy,
- maximum core power,
- power pulse width.

The sensitivities S_x to the quantities x were obtained from 3-D pin-by-pin calculations for different quantities x using the RELAP-BARS coupled code. The uncertainties in the neutronic and thermal-hydraulic quantities $\delta x/x$ were estimated by engineering judgement, using evidence from available references and validation results for the BARS code.

3.2 Analysis for Central Rod Ejection

The uncertainty analysis in safety parameters was carried out for the TMI-1 PWR with a high burnup core. The reactor of 2772 MW rated power, having one-eight symmetry, contains fuel assemblies with fuel burnup ranged from 23 up to 58 GWd/t (at the end of the cycle) as shown in Figure 2.1. The REA was defined for the central control rod at HZP with an ejection time of 100 ms (Ref. 5). The reference (without scram) transient duration was 2.5 s. Figure 3.1 shows the core power and the reactivity as a function of time for the reference case up to the end of the transient (2.5 s).

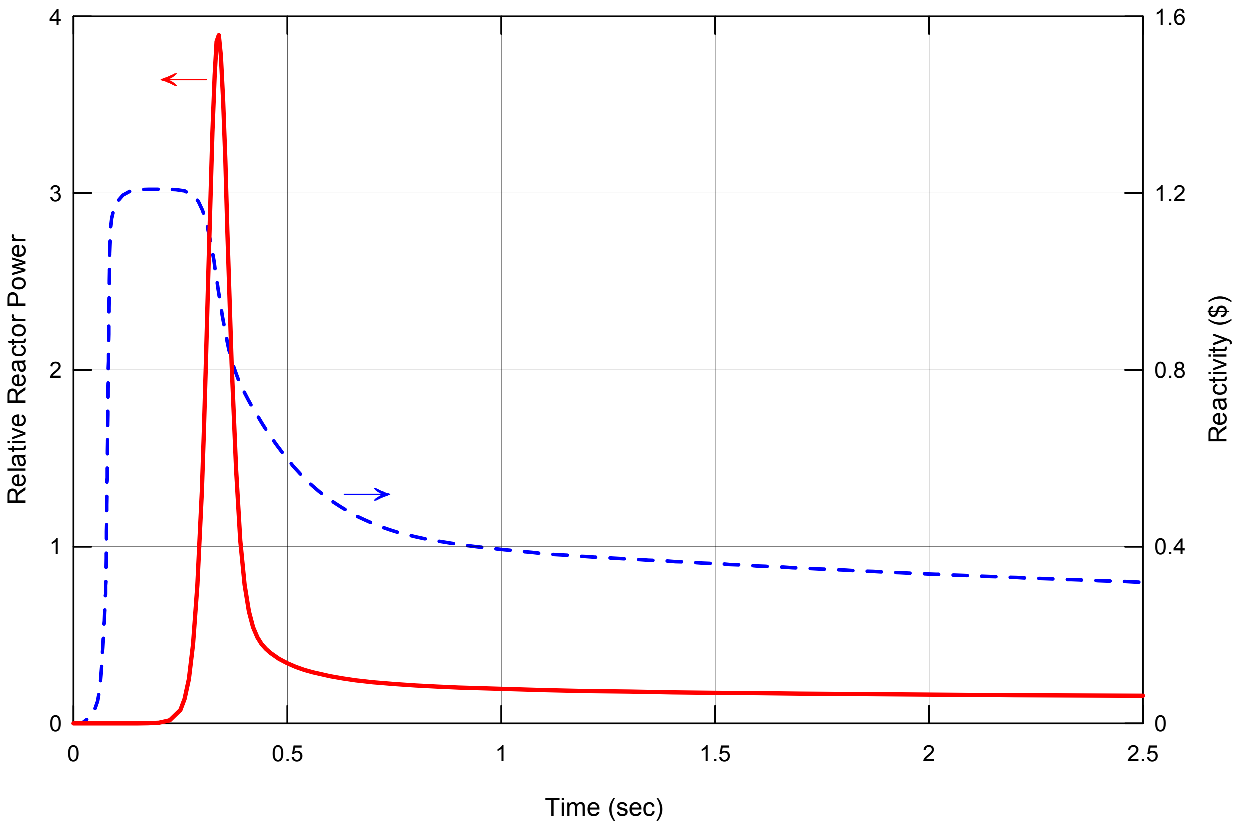

Figure 3.1 Core Power and Reactivity vs. Time

The following values of the key parameters were obtained as reference ones:

- ejected rod worth – 1.21β;
- peak power – 398.6% of rated power;
- time of peak – 336 ms;
- power pulse width – 61.9 ms;
- maximum fuel pellet enthalpy – 37.6 cal/g;
- maximum increase in fuel pellet enthalpy – 20.6 cal/g.

In the reference transient the local fuel enthalpy reaches its maximum value at the end of the transient. To estimate a real time when the fuel enthalpy reaches its maximum, an additional transient with scram was calculated. In this transient it was supposed that reactor scram occurs with 0.45 s delay at 35% of rated power. Control rods movement during the scram was modeled with a speed of 155.8 cm/s (Ref. 2).

Figure 3.2 shows the fuel pellet enthalpy increment as a function of time for both reference and additional transients. The peak of 17.4 cal/g in the fuel enthalpy increment occurs at the time of 0.785 s for the transient with scram. The reference transient overestimates the fuel enthalpy by less than 0.5% at that moment.

The following neutronic and thermal-hydraulic quantities were taken into consideration during the uncertainty analysis:

- reactivity worth of the ejected rod (ρ),
- delayed neutron precursor fraction (β),
- fuel temperature (Doppler) reactivity coefficient (α_d),
- moderator density reactivity coefficient (α_m),
- pellet heat capacity (C_p),
- gap conductance (h_g),
- pellet conductivity (K_f),
- clad-moderator heat transfer coefficient (h_w),
- fraction of energy deposited directly in the moderator (γ),
- radial power peaking factor for the pellet (F_p).

Sensitivity S_x was obtained as a result of corresponding calculation of the transient with perturbed quantities. Different variations of these neutronic and thermal-hydraulic quantities from their reference values were used. The reference value of the delayed neutron precursor fraction was perturbed by –10%; the value of the Doppler reactivity coefficient was changed by –9%; the value of the moderator density reactivity coefficient was increased by 2.1 times. All table data for pellet heat capacity, gap conductance, pellet conductivity, and clad-moderator heat transfer coefficient were increased by 10%. The energy deposited directly in the moderator was not taken into account in the reference transient. To estimate the sensitivity to this quantity, the values of 2% and 5% were considered for the fraction of energy deposited in the moderator. In the reference calculation the radial power distribution in the pellet was assumed as uniform one. To estimate the sensitivity to this distribution, the parabolic power distribution was considered with the peaking factor of 1.05.

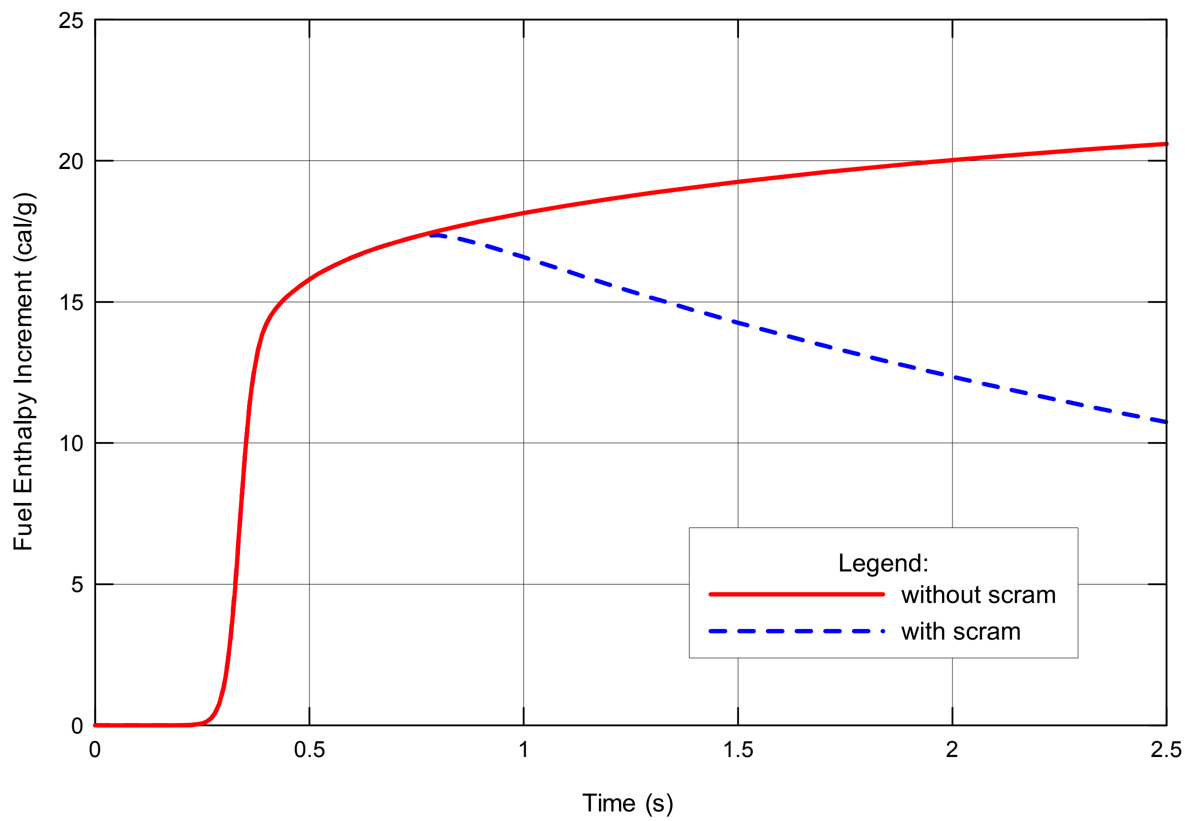

Figure 3.2. Fuel Pellet Enthalpy Increment vs. Time

The most important quantity is the reactivity worth of ejected control rod. The sensitivity of the maximum fuel enthalpy to the control rod worth strongly depends on both reference and perturbed values of the rod worth. To obtain the conservative estimation for this sensitivity it is necessary to use the perturbation determined by engineering judgement of the uncertainty in the rod worth instead of arbitrary small perturbation. Unfortunately, the BARS pin-by-pin neutronic model does not allow increasing the rod worth by more than 4% against its reference value (1.21β). To consider larger perturbation in the control rod worth the following formula can be applied to the sensitivity of the fuel enthalpy to the control rod worth:

$$S_\rho = S_{\rho 1}(1-\beta/\rho)/(1-\beta/\rho_1) \qquad (19)$$

where S_ρ is the sensitivity for the required perturbed value of the rod worth (ρ) and $S_{\rho 1}$ is the sensitivity for the perturbed value ρ_1 ($\rho > \rho_1$). $S_{\rho 1}$ was obtained from RELAP-BARS calculation with the rod worth increased by 3.7% in comparison with the reference value ($\rho_0 = 1.21\beta$). This formula was derived using a simple expression for the energy deposition obtained in a frame of the Nordheim-Fuchs approximation (Ref. 10). The formula was checked using another value for ρ_1 obtained by increasing the reference value ρ_0 by 2.4%. Both results are very close.

The following values were obtained for the uncertainties in the neutronic and thermal-hydraulic quantities:

- reactivity worth of the ejected rod – 15%;
- delayed neutron precursor fraction – 5%;
- fuel temperature reactivity coefficient – 15%;
- moderator density reactivity coefficient – 5%;
- pellet heat capacity – 8%;
- gap conductance – 110%;
- pellet conductivity – 25%;
- clad-moderator heat transfer coefficient – 10%;
- fraction of energy deposited in the moderator – 20%;
- radial power peaking factor for the pellet – 5%.

The uncertainty in the calculated rod worth was estimated as equivalent to two standard deviations based on the data presented in Ref. 10. The uncertainties in the delayed neutron precursor fraction, the Doppler coefficient, and pellet heat capacity were taken from Ref. 10. The maximum uncertainty in the Doppler coefficient, obtained from the BARS validation results (Ref. 12) does not exceed the uncertainty estimated in Ref. 10 using engineering judgement. The uncertainty in the moderator density reactivity coefficient was obtained from the BARS validation results (as a result of comparisons with precise Monte Carlo calculations) (Ref. 12). The uncertainty in gap conductance was estimated taking into account that the gap closure could take place. It was obtained by a calculation of the transient with the closed gap. The uncertainty in pellet conductivity was estimated using the data from handbook (Ref. 13), and the uncertainty in the clad-moderator heat transfer coefficient was taken from (Ref. 14). The uncertainties in the fraction of energy deposited directly in the moderator and in the radial power peaking factor for the pellet were estimated using engineering judgement.

It should be noted that unlike the maximum core power and power pulse width, the maximum fuel pellet enthalpy is a local parameter. So, the uncertainty in the local power should be taken into account to estimate the uncertainty in the fuel enthalpy together with above-mentioned quantities. A perturbation in local power is not calculated by RELAP-BARS directly without perturbations other quantities. Therefore, the approach proposed in Ref. 10 was used to estimate contribution of the uncertainty in local power to the uncertainty in fuel pellet enthalpy. If one assumes that the increase in fuel pellet enthalpy is proportional to the local power form factor F_L, then the contribution of the uncertainty in local power to the uncertainty in fuel enthalpy can be considered as the addition of $(\delta F_L / F_L)^2$ to the formula (18). F_L is defined as the fuel pellet power divided by the total core power. Based on the analysis carried out in Ref. 10, the uncertainty of 8% was taken for F_L.

Table 3.1 presents the calculational results for the sensitivity of fuel pellet enthalpy.

Table 3.1. Sensitivity of Fuel Pellet Enthalpy

Quantity	PARCS	BARS (at = 0.785 s)		BARS (at = 2.5 s)	
(x)	S_x	S_x	$(S_x)^2(\delta x/x)^2$	S_x	$(S_x)^2(\delta x/x)^2$
ρ	5.5	7.14	1.147	4.36	0.428
β	-4.0	-3.05	0.023	-1.34	0.004
α_d	-1.0	-0.90	0.018	-0.77	0.013
α_m	-	-0.18	$< 10^{-3}$	-0.39	$< 10^{-3}$
C_p	0.9	0.04	$< 10^{-3}$	0.15	$< 10^{-3}$
h_g	-	-0.09	0.010	-0.12	0.017
K_f	-	-0.04	$< 10^{-3}$	-0.20	0.003
h_w	-	-0.07	$< 10^{-3}$	-0.08	$< 10^{-3}$
γ	-	-0.03	$< 10^{-3}$	-0.02	$< 10^{-3}$
F_p	-	-0.20	$< 10^{-3}$	-0.23	$< 10^{-3}$

The RELAP-BARS results for the sensitivity of fuel enthalpy S_x and for contributions of each quantity x to the uncertainty in fuel enthalpy $(S_x)^2(\delta x/x)^2$ are presented at two time moments: the time of the maximum fuel enthalpy in the transient with scram (t=0.785 s) and for the end of the transient (t=2.5 s). For comparison, corresponding results for the sensitivity of fuel enthalpy obtained using the PARCS code (Ref. 10) are presented in Table 3.1 too. The results demonstrate that the sensitivity of fuel enthalpy to the most of quantities strongly depends on time because of non-adiabatic nature of the transient. Maximum contribution to the uncertainty in fuel enthalpy is due to the uncertainty in rod worth.

Qualitatively, the RELAP-BARS results are agreed with the PARCS ones. However, the PARCS results give conservative estimation for the sensitivity to the most of the quantities in comparison with the RELAP-BARS results, because the adiabatic approximation was used in the PARCS calculations. Table 3.1 shows larger value of the sensitivity to rod worth obtained using BARS at t = 0.785 s, because a perturbation of +15% in rod worth was considered using Eq. (19) instead of a very small perturbation used in PARCS. Note that the BARS gave the value of 5.14 for the sensitivity for a perturbation in rod worth of +3.7% and the value of 4.93 for a perturbation of +2.4%.

The resulting uncertainty in the maximum fuel pellet enthalpy (the transient with scram) obtained using the BARS calculations is 110% for a rod worth of 1.2β. The uncertainty in fuel pellet enthalpy is 69% at the end of the reference transient.

The RELAP-BARS calculational results for the sensitivity of the maximum core power and power pulse width are given in Table 3.2.

Table 3.2. Sensitivity of Maximum Core Power and Power Pulse Width

Quantity (x)	Maximum Core Power		Pulse Width	
	S_x	$(S_x)^2(\delta x/x)^2$	S_x	$(S_x)^2(\delta x/x)^2$
ρ	13.87	4.328	-4.98	0.558
β	-10.77	0.290	3.09	0.024
α_d	-0.97	0.021	< 0.01	$< 10^{-3}$
α_m	-0.01	$< 10^{-3}$	-0.02	$< 10^{-3}$
C_p	1.05	0.007	0.01	$< 10^{-3}$
h_g	< 0.01	$< 10^{-3}$	< 0.01	$< 10^{-3}$
K_f	< 0.01	$< 10^{-3}$	< 0.01	$< 10^{-3}$
h_w	-0.01	$< 10^{-3}$	-0.01	$< 10^{-3}$
γ	-0.03	$< 10^{-3}$	-0.01	$< 10^{-3}$
F_p	< 0.01	$< 10^{-3}$	< 0.01	$< 10^{-3}$

The most contribution to the total uncertainty in the maximum core power and power pulse width is due to the uncertainty in rod worth as well as in case with fuel pellet enthalpy. Contributions of other quantities to the resulting uncertainties are very small. The resulting uncertainties were estimated as 216% in the maximum reactor power and 76% in power pulse width.

3.3 Effect of Initial Core Power

To analyze the effect of initial core power on key safety parameters, a calculation of the ejection of the central rod in the TMI-1 PWR starting from 33% of rated power was carried out using RELAP-BARS. To simplify a comparison of the results for HZP and non-zero power conditions, the same maximum value of 1.2β for the reactivity was considered in REA from 33% of rated power. The same RELAP input deck was used in the RELAP-BARS calculation as in the HZP case. To reach a criticality for the initial steady state, an additional withdrawal of control rods at the core periphery was done in the BARS input deck. No other changes were done in the HZP input deck.

Figures 3.3 and 3.4 show the reactor power and reactivity as a function of time for both HZP and 33% of rated power cases. In the last case the core power reaches its maximum value of approximately 14% of rated power at about 0.13 seconds. This peak value by more than 3.5 times exceeds corresponding value for the zero power case under the same maximum value of reactivity.

The reasons for this very large difference are the following.

- The decrease of 80% in the Doppler reactivity coefficient for the non-zero power case in comparison with the HZP one. This produces the factor of 1.8 in the resulting difference.
- The increase of 3% in the “net” (without feedback) reactivity inserted by the control rod for the non-zero power case in comparison with the HZP one. Note that in the HZP case the “net” reactivity inserted by the control rod and the maximum reactivity are the same. This increase produces the factor of 1.55.
- The “net” effect of initial power on peak power. This produces the factor of 1.15 in the resulting difference.
- The increase of 10% in pellet heat capacity for the non-zero power case in comparison with the HZP one. This produces the factor of 1.1.

Unlike the HZP case, in the non-zero power case the effect of feedback appears during the ejection of the control rod. This provides power pulse behavior as faster and sharper compared with the HZP case.

Figure 3.5 shows assembly averaged radial power at three states of the core: at the initial steady state (0 s), at the time of the peak power (0.13 s), and at the end of the transient (2.5 s). Unlike the HZP case, significant deformations in radial power distribution take place after the rod ejection in the non-zero power case. Assembly powers differ up to 14.6% at the time of the peak power and at the end of the transient.

Figure 3.6 shows fuel enthalpy in the hottest fuel pellet as a function of time for two assemblies: K10 and H9. Up to the time of 1.6 s the maximum value of enthalpy occurs in the pellet located in assembly K10, but at the end of the transient assembly H9 contains the pellet with the maximum enthalpy. Change in the hottest pin location takes place due to power redistribution during the transient. This phenomenon can lead to some difficulties in a prediction of the hottest pin using assembly-by-assembly approach together with the pin reconstruction procedure to calculate fuel pellet enthalpy.

Table3.3 summarizes the calculation results of the effect of initial power on parameters of the accident.

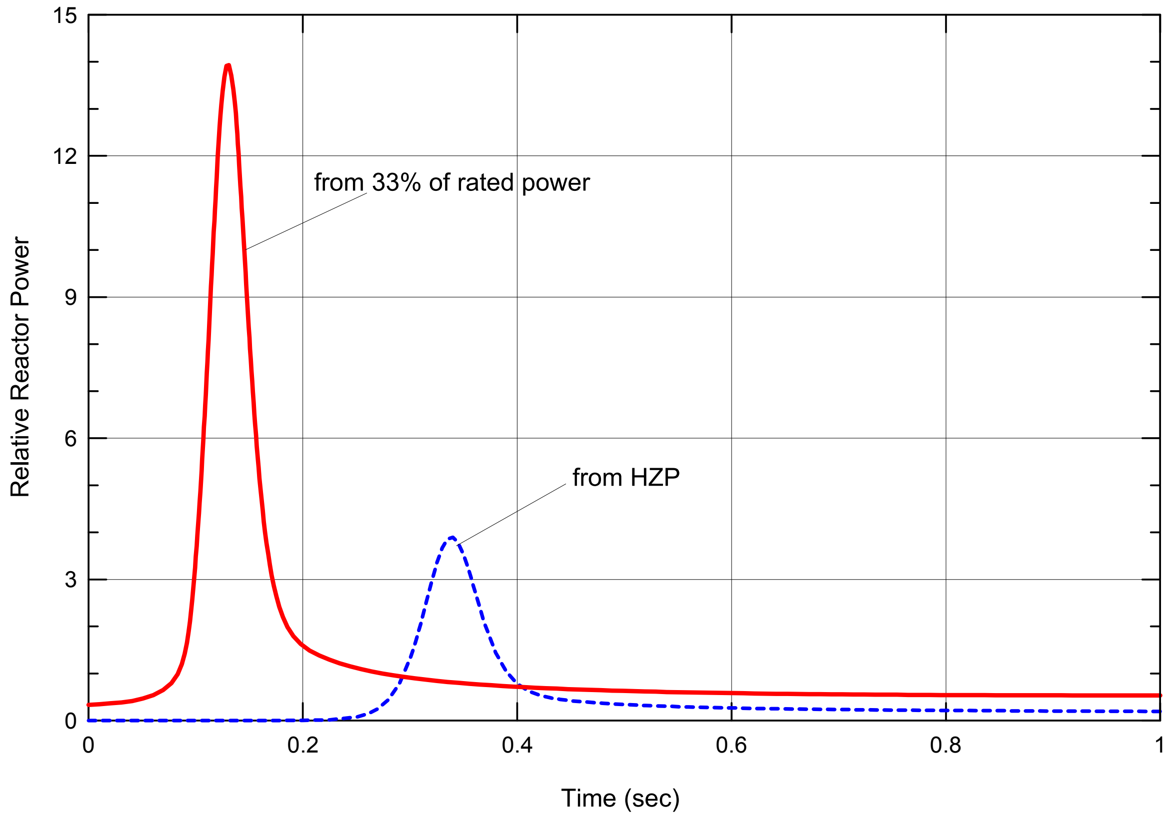

Figure 3.3. Reactor Power vs. Time

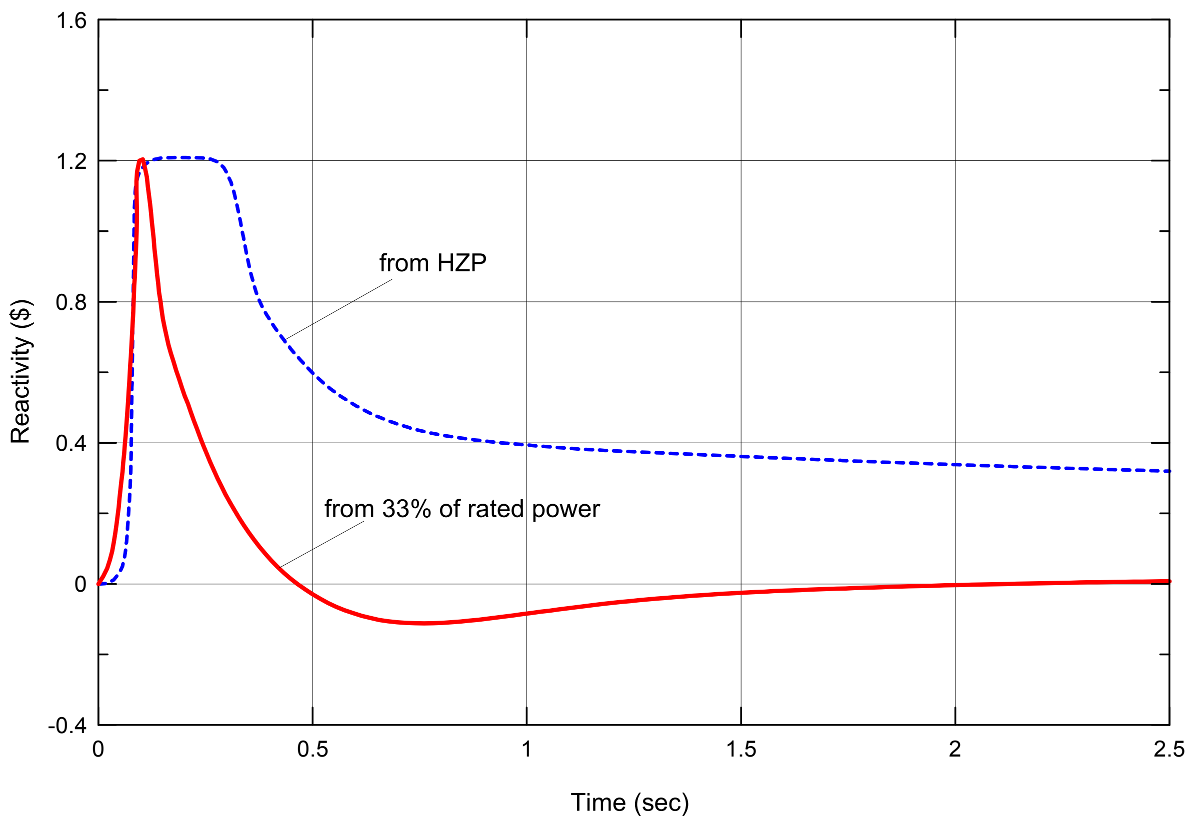

Figure 3.4. Reactivity vs. Time

	8	9	10	11	12	13	14	15
H	0.213 1.936 1.690	1.169 2.514 2.227	1.298 1.826 1.654	1.458 1.687 1.580	0.647 0.641 0.636	0.974 0.830 0.878	0.747 0.589 0.646	0.391 0.299 0.333
K		1.139 1.936 1.726	1.613 2.133 1.949	1.242 1.383 1.305	1.247 1.202 1.202	0.664 0.561 0.595	1.141 0.893 0.984	0.471 0.361 0.402
L			1.278 1.502 1.398	1.445 1.495 1.443	1.157 1.051 1.071	1.355 1.112 1.191	1.189 0.927 1.021	0.438 0.334 0.372
M				0.704 0.665 0.669	1.217 1.040 1.091	1.021 0.817 0.883	0.785 0.608 0.671	
N					0.664 0.537 0.579	1.062 0.826 0.908	0.499 0.383 0.424	
O			at t = 0 s → at t = 0.13 s → at t = 2.5 s →			0.607 0.464 0.514		

Figure 3.5. Assembly Averaged Power at Three States of the Core

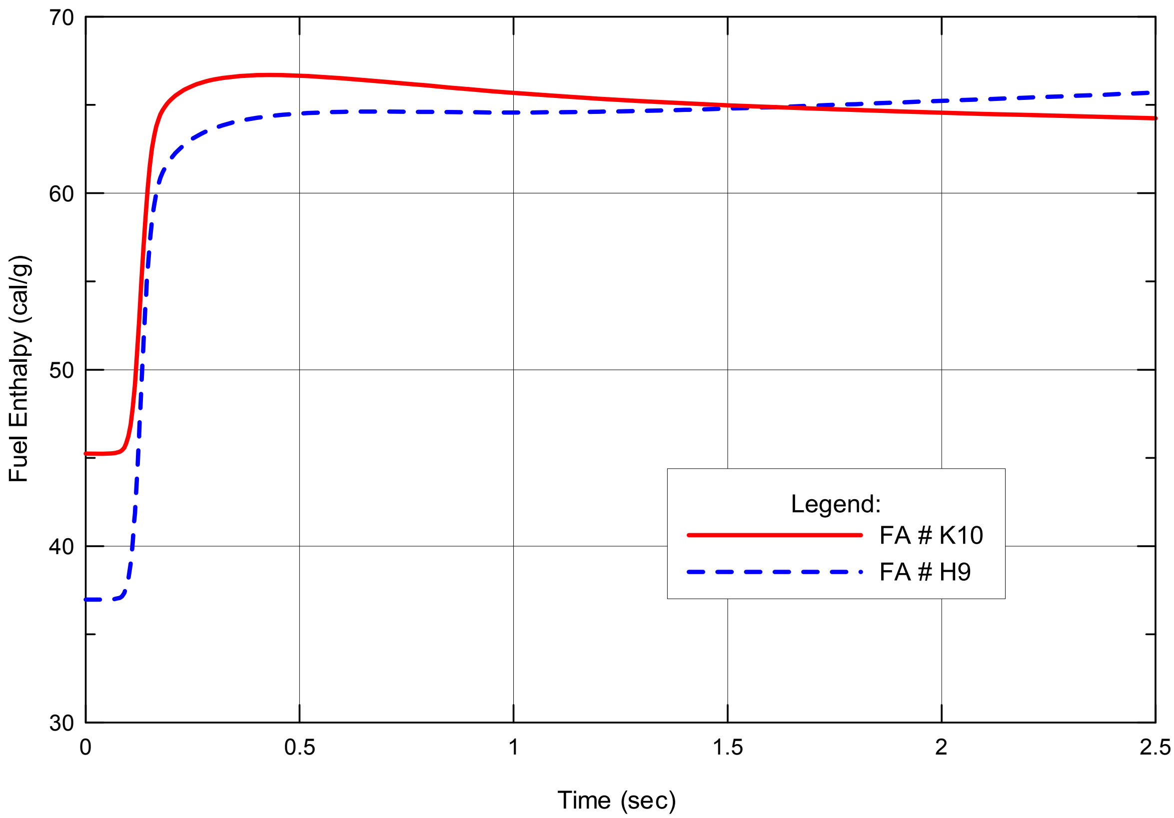

Figure 3.6. Fuel Enthalpy in the Hottest Pellet vs. Time

Table 3.3. REA Parameters in Comparison with the HZP Case

Parameter	From 33% of rated power	From HZP
Maximum inserted reactivity (β)	1.22	1.21
Peak power of the core (GW)	38.7	11.0
Time of peak power (ms)	130	336
Power pulse width (ms)	44	62
Position of the hottest assemblies	K10 and H9	H9
Peak power of the fuel pin (MW)	2.82	0.835
Maximum fuel pellet enthalpy (cal/g)	66.7	37.6
Maximum fuel enthalpy increment (cal/g)	28.7	20.6
Minimum of coolant outlet density (g/cc)	0.691	0.755

Comparison between the HZP case and the REA from 33% of rated power shows that the difference in the maximum fuel enthalpy increment is about 40% and the maximum fuel pellet enthalpies differ by about 29 cal/g (37.6 versus 66.7 cal/g).

4 CONCLUSIONS

This study was undertaken to analyze spatial effects during rod ejection accidents. If the ejected rod worth is sufficient to reach prompt critical, i.e. greater than β, the result is a fast power excursion terminated by negative reactivity feedback from the increase in fuel temperature. This event is of interest from the point of view of prediction of the maximum increase in fuel enthalpy during the accident. Although, as numerous steady-state calculations show, the maximum value of control rod worth scarcely exceeds 1β in most PWRs, such an accident is frequently considered in NPP safety analyses with a conservatively increased value of the ejected rod worth.

A key parameter of interest in an NPP safety analysis is the peak local fuel enthalpy, which establishes the acceptance criterion for unacceptable fuel damage in reactivity initiated accidents. It is well-established that spatial effects play an important role in the REA consequences, in particular, the core peak power and energy deposition, which is approximately the fuel enthalpy rise under an adiabatic assumption (no heat transfer from the fuel to the coolant). Using simplified analytical approximations it is possible to establish relationships between the major parameters of interest and spatial effects. To characterize them, the power peaking factors, F_q and F_q' are used: the former is related to the pin-by-pin representation of the core power, and the latter to the assembly-by-assembly one.

Localized spatial effects impact the REA parameters in two different ways. On the one hand, the higher the power peaking factor, the higher the local fuel enthalpy. On the other hand, a higher value of F_q tends to slow down the total energy deposition in the core and, as a result, to mitigate the fuel enthalpy increase. This is due to the fact that the fuel and moderator feedback is strongest in the hottest regions of the reactor core and reduces the peak power and reactivity.

In this study an analysis of REAs was carried out using the RELAP5–BARS code (Ref. 1), which uses a 3-D pin-by-pin neutronic and assembly-by-assembly thermal-hydraulic simulation of a LWR. Four REAs with ejection of the central or peripheral control rod and at EOC or BOC initial conditions were analyzed using a PWR model based on TMI-1. The same EOC PWR model was used for a previous study of the REA using different methods from U.S.A., France, and Russian Federation (Ref. 5).

To provide identical initial conditions the worth of an ejected control rod was artificially fitted to 1.21β for all cases. Duration of the transient was limited to 2.5 s. An assembly-average representation of fuel and coolant parameters with 24 nodes in an axial direction was used to treat the core thermal-hydraulics. A separate heat structure was chosen to represent the hottest fuel pin in the reactor core (the coolant parameters were the same as for the fuel assembly where the hottest pin was located).

The results showed that peak power varied from 4.4 to 37.5 GW. In the cases with ejection of the peripheral rod, the peak power was lower compared with ejection of the central rod by a factor of 2.5 at EOC and 2.9 at BOC. An inverse relationship was found for the power peaking factors. The maximum assembly-average fuel temperatures were very close (within about 1 K) for the BOC cases. Corresponding values for the maximum fuel enthalpy increase were approximately 25.5 cal/g. For the EOC cases those values differed by 2 cal/g (18.9 and 16.9 cal/g for EOC center and EOC periphery, respectively).

Thus, from the point of view of the assembly-by-assembly representation, the central rod ejection accidents with rather small power peaking factors resulted in slightly higher values of the maximum fuel enthalpy increase. On the contrary, the pin-by-pin representation showed that the peak local fuel enthalpy was higher for the peripheral REAs with the highest power peaking factors. In the EOC cases, a higher value of the peak enthalpy was due to the fact that the hottest fuel pin was found in Assembly N13 (see Figure 2.5) diagonally adjacent to the hot assembly M12. This fact indicates that defining the hottest pin location is problematic. In this case, the incorrect definition of the hottest pin location using an assembly-by-assembly approach, can lead to a 15% underestimation of the peak local enthalpy rise. Therefore, this should be taken into account in an uncertainty analysis of reactivity initiated accidents.

The point kinetics approximation within the Nordheim-Fuchs model results in simple relationships for the peak power, total energy deposition and, with certain modifications, the power peaking factor. It was found that in the framework of this model the peak power and total energy deposition are inversely proportional to the power peaking factor. Thus, if it is assumed that the peaking factor for fuel enthalpy increase coincides with that for power, then it can be expected that the maximum assembly-average fuel enthalpy increase is practically independent of spatial effects.

In spite of the fact that the Nordheim-Fuchs model is valid only within a narrow time interval limited by the power pulse area, this simplified approach (with the point kinetics parameters evaluated in advance) may be successfully used, in particular, for estimation of the major parameters of REAs.

Another important problem in REA analysis is the uncertainty in prediction of the rod worth by different calculational methods. As was found during this study, the BARS results for the rod worths were always higher compared with those calculated by the PARCS code. The most significant difference occurs for the peripheral rod N12 (see Figures 2.1 and 2.2) nearest to the reflector region. At the EOC initial conditions this difference reaches 35%. The suspected reason for this discrepancy is the different treatment of the reflector boundary conditions in BARS vs nodal diffusion codes such as PARCS. More research would be needed with, for example, more precise calculational methods in order to resolve this difference.

As the steady-state calculations of the rod worths show, a rod worth of 0.91β—below prompt critical--seems to be the highest one. Thus, to provide the value of 1.2β for rod worth, it is necessary to artificially adjust the neutronics parameter of the ejected rod. Another, more realistic, approach is to assume that there is a withdrawn rod near the ejected control rod. For instance, in the case of ejection of the peripheral rod N12 (with "stuck" rod M11) the inserted reactivity value may reach 1.74β at EOC HZP conditions.

In summary, the objective of this study was to understand the role of spatial effects on the outcome of different rod ejection accidents. The influence of spatial effects may be of interest not only in an analysis of reactivity initiated events, but also in interpretation of in-pile burst tests aimed to understand fuel rod behavior under severe accidents. The present study has also looked at the effect of the calculational approach (pin-by-pin against assembly-by-assembly) on the major outcome of an REA – the peak local enthalpy increase.

The uncertainty analysis for the PWR central rod ejection accident starting from the HZP conditions carried out with the RELAP5-BARS code showed that the uncertainties in the key parameters of the accident would be determined to a large extent by the uncertainty in ejected rod worth. For a rod worth of 1.2β with an uncertainty of 15% (corresponding to two standard deviations), the uncertainty in local fuel enthalpy was estimated as 110%, the uncertainty in the maximum core power as 216%, and the uncertainty in power pulse width as 76%.

The results demonstrated the non-adiabatic nature of the transient and showed that the sensitivity of fuel enthalpy to most of the neutronic and thermal-hydraulic quantities strongly depends on time. Qualitatively, the RELAP5-BARS results are in agreement with the PARCS ones.

The comparative study of the accident starting from 33% of rated power showed strong dependence of a number of the REA parameters on initial core power. Under the same rod worth of 1.2β, the peak power in the transient from 33% of rated power was 3.5 times greater than that in the transient from HZP. Unlike the HZP case, a change in the hottest fuel pin location takes place due to power redistribution during the transient from the non-zero power. This phenomenon can lead to some difficulties in predicting the hottest pin using the assembly-by-assembly approach with pin reconstruction to calculate fuel pellet enthalpy. In comparison with the HZP case, the REA from 33% of rated power leads to an increase in the maximum fuel pellet enthalpy to 66.7 cal/g.

5 REFERENCES

1. A. Avvakumov, V. Malofeev, and V. Sidorov, "Analysis of Pin-by-Pin Effects for LWR Rod Ejection Accident," NUREG/IA-0175, 2000.

2. K. N. Ivanov, et al., "Pressurized Water Reactor Main Steam Line Break (MSLB) Benchmark; Volume I: Final Specifications," OECD Nuclear Energy Agency, NEA/NSC/DOC(99)8, April 1999.

3. N. K. Todorova and K. N. Ivanov, "Project Report on Task 1 of BNL Sub-Contract "Core Model – PARCS/RELAP5," The Pennsylvania State University, 2000 (available at www.nrc.gov in NRC's public document system, ADAMS, as ML070660645).

4. A. Avvakumov, et al., "3-D Pin-by-Pin Modeling of Rod Ejection RIA in VVER-1000," Nuclear Safety Institute of Russian Research Centre "Kurchatov Institute", Report No. 90-12/1-33-97, 1997 (available at www.nrc.gov in NRC's public document system, ADAMS, as ML070670258).

5. D. J. Diamond, et al., "Intercomparison of Results for a PWR Rod Ejection Accident," Nuclear Engineering and Design, 208, 2001.

6. G. Bell and S. Glasstone, "Nuclear Reactor Theory," Van Nostrand Reinhold Company, 1970.

7. T. J. Downar et al., "PARCS: Purdue Advanced Reactor Core Simulator," Proc. International Conference on the New Frontiers of Nuclear Technology: Reactor Physics, Safety and High-Performance Computing (PHYSOR 2002, Seoul, Korea), American Nuclear Society, October 2002.

8. J.-J. Lautard, S. Loubière, C. Fedon-Magnaud, "CRONOS2, A Modular Computational System for Neutronic Core Calculations," IAEA Specialists Meeting on Advanced Calculational Methods for Power Reactors, Cadarache, France, IAEA-TECDOC-678, 1990 (available at www.nrc.gov in NRC's public document system, ADAMS, as ML070670239).

9. B. P. Bromley, Memo to D. J. Diamond, Brookhaven National Laboratory, May 2, 2001 (available at www.nrc.gov in NRC's public document system, ADAMS, as ML062140704).

10. D.J. Diamond, A.L. Aronson, and C.Y. Yang, "A Qualitative Approach to Uncertainty Analysis for the PWR Rod Ejection Accident," Transactions of the American Nuclear Society, 83, 416, 2000.

11. "RELAP5/MOD3.2 Code Manual," NUREG/CR-5535, 1995.

12. A. Avvakumov, V. Malofeev, "Validation of a Pin-by-Pin Neutron Kinetics Method for LWRs," Proceeding of the International Twenty-Sixth Water Reactor Safety Information Meeting, Bethesda, Maryland, October 1998, NUREG/CP-0166, Volume 3, June 1999.

13. P.L. Kirillov, Y.S. Yuriev, V.P Bobkov, "Handbook on Thermal-Hydraulic Calculations," in Russ., Energoatomizdat, Moscow, 1990.

14. I.I. Novikov, K.D. Voskresensky, "Applied Thermal-Dynamics and Heat Transfer," in Russ., Gosatomizdat, Moscow, 1961.

APPENDIX A

CALCULATIONAL RESULTS FOR A REA WITH INCREASED ROD WORTH

As it was above mentioned, the BOC delayed neutron fraction was approximately 21% higher compared with that at the EOC conditions (632 pcm against 521 pcm). This means that at the same relative rod worth expressed in terms of β, there are two different absolute values of the rod worth at BOC and EOC. For instance, for a 1.21β rod worth the absolute values are 631 pcm and 765 pcm at EOC and BOC, respectively. In this respect it would be interesting to compare the results for EOC REA with the same absolute value of the rod worth as at BOC, i.e. 765 pcm (1.47β).

This section contains the calculational results of a REA with ejection of the central rod with increased worth obtained by the RELAP–BARS code. The absolute value of the rod worth corresponds to that presented in Table 2.2 for the BOC cases, i.e. 765.7 pcm or 1.47β in terms of the EOC delayed neutron fraction. The reactor model and the accident scenario were the same as described in Section 2. To provide required 1.47β, the initial arrangement of the control rod banks was changed. As was found it was impossible to obtain such a high reactivity only by changing neutronic parameters of the ejected rod. For this reason, four control rods of Bank 2 located at Assembly K9 diagonally adjacent to Assembly H8 were partly inserted before the REA (see Figure 2.1). Then they were also withdrawn together with the ejected rod H8 with the same speed.

Table A.1 summarizes the calculational results of 1.47β EOC transient with ejection of the central control rod. Figures A.1 and A.2 show the following parameters as a function of time of the transient: the core power, reactivity, fuel temperature, and fuel enthalpy increase for the hottest fuel pin.

The power pulse, as can be seen in Figure A.1, is very narrow, the pulse width is less than 30 ms. The power excursion produces rapidly the core heat-up, and due to the negative fuel and moderator temperature feedback, is terminated. As a result of the strong feedback, the reactivity drops up to 0.06β (against 0.3-0.4β in 1.21β transients) at about 0.7s. After a while the reactivity becomes to rise as a result of the positive reactivity insertion due to the core cooldown. (This effect was not observed during the 1.21β REA analysis, nevertheless, as was reported in Ref. 5, the Doppler and moderator reactivity effects were of the same order.

It is obvious that sooner or later the negative moderator feedback component becomes to decrease due to forced circulation of the coolant with the core inlet temperature of 551 K.)

As can be seen in Figure A.2 the fuel temperature/enthalpy reaches a peak value at about 0.5 s, then gradually decreases. The maximum fuel pellet temperature is 995 K, which corresponds to the enthalpy increase of 33 cal/g. The last value is higher by about 60% in comparison with Case EOC Centre, i.e. 1.21β REA (see Table 2.2). This is in contrast to the simplified estimation: according to Eq. 3 it should be expected at least twice as high (or more precisely, about 46 cal/g).

Table A.1. Calculational Results for 1.47β EOC REA

Parameter	Value
Ejected Rod Worth (pcm / β)	765.7 / 1.4695
Peak Power (GW / % Nominal)	48.83 / 1762
Time of Peak Power (ms)	206.4
Power Pulse Width (ms)	29.5
Maximum Core-Average Fuel Temperature (K)	610.6
Maximum Fuel Assembly Temperature (K)	960.5
Maximum Fuel Pin Temperature (K)	995.1
Maximum Assembly Enthalpy Increase (cal/g)	30.27
Maximum Pin Enthalpy Increase (cal/g)	32.96
Time of Maximum Pin Enthalpy Increase (ms)	507.0
Position of the Hottest Assembly	H9
Position of the Hottest Fuel Pellet (Axial Layer)	H9 (Node 22)

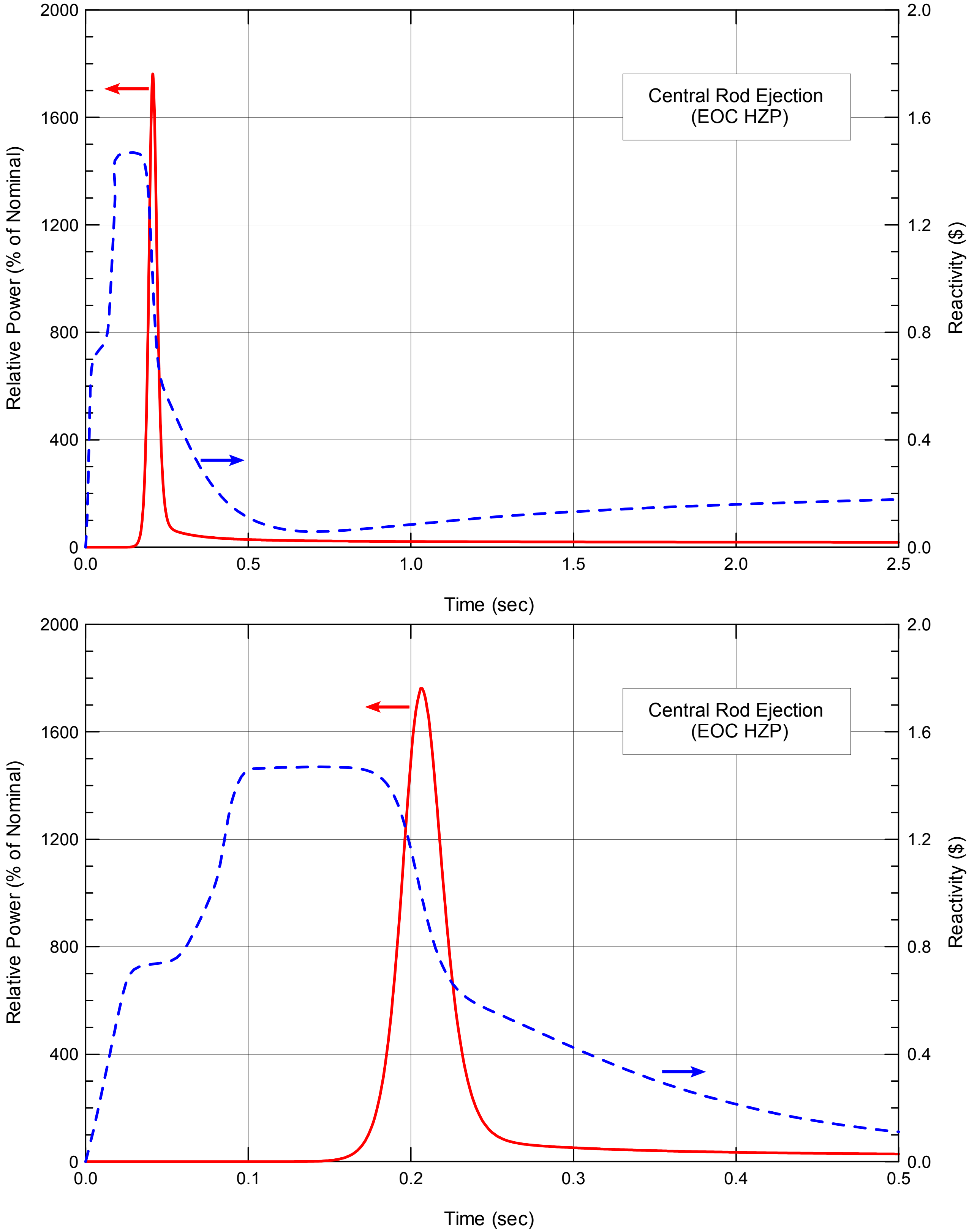

Figure A.1. Power and Reactivity vs. Time

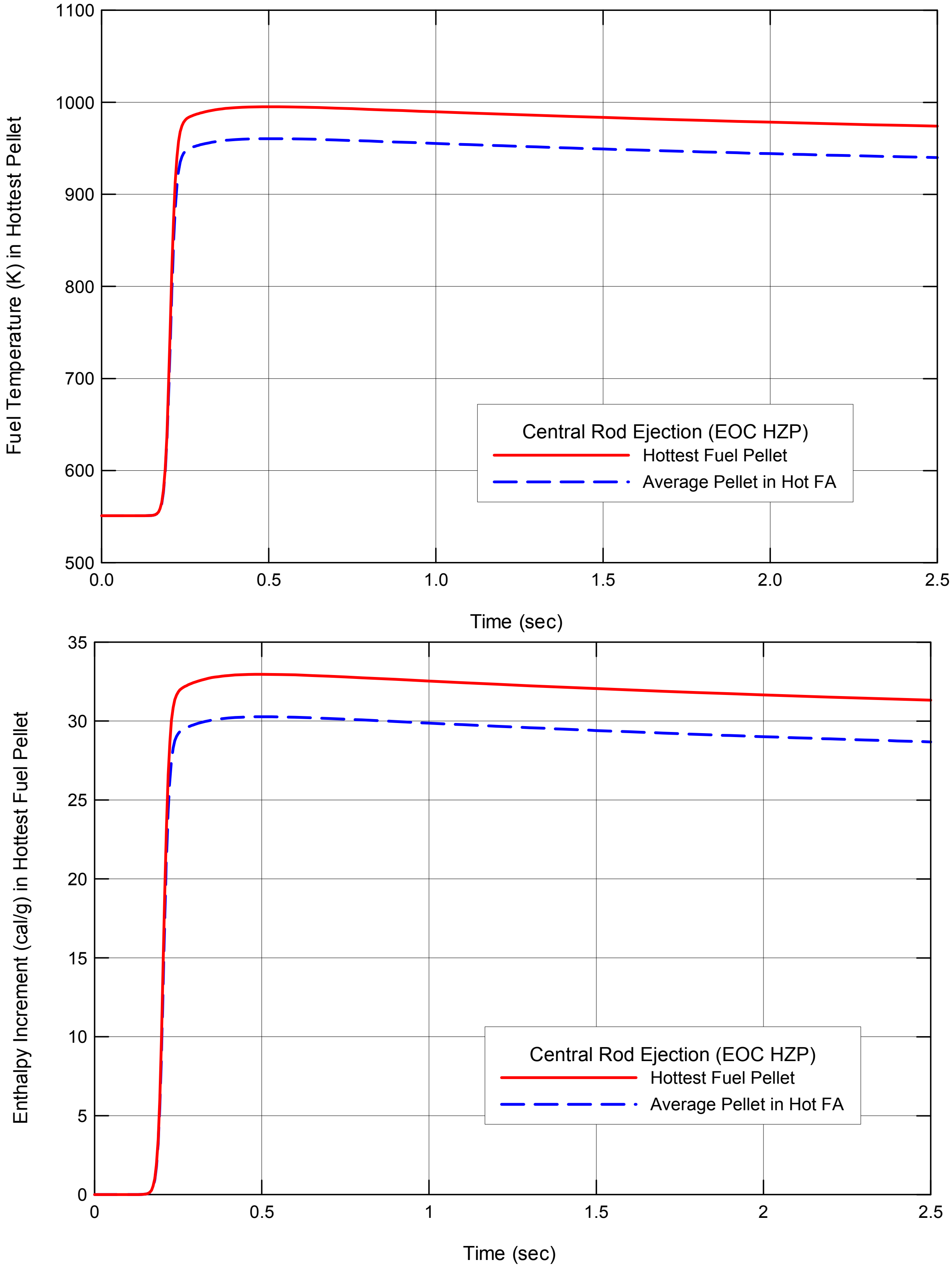

Figure A.2. Fuel Temperature and Enthalpy in Hot Pins vs. Time

NRC FORM 335
(9-2004)
NRCMD 3.7

U.S. NUCLEAR REGULATORY COMMISSION

BIBLIOGRAPHIC DATA SHEET

(See instructions on the reverse)

1. REPORT NUMBER
(Assigned by NRC, Add Vol., Supp., Rev., and Addendum Numbers, if any.)

NUREG/IA-0215

2. TITLE AND SUBTITLE

Spatial Effects and Uncertainty Analysis for Rod Ejection Accidents in a PWR

3. DATE REPORT PUBLISHED

MONTH	YEAR
September	2007

4. FIN OR GRANT NUMBER

Y6723

5. AUTHOR(S)

A. Avvakumov, V. Malofeev, V. Sidorov

6. TYPE OF REPORT

7. PERIOD COVERED *(Inclusive Dates)*

2001-2005

8. PERFORMING ORGANIZATION - NAME AND ADDRESS *(If NRC, provide Division, Office or Region, U.S. Nuclear Regulatory Commission, and mailing address; if contractor, provide name and mailing address.)*

Russian Research Center - Kurchatov Institute
Moscow 123182
Russia

9. SPONSORING ORGANIZATION - NAME AND ADDRESS *(If NRC, type "Same as above"; if contractor, provide NRC Division, Office or Region, U.S. Nuclear Regulatory Commission, and mailing address.)*

Division of Risk Assessment and Special Projects
Office of Nuclear Regulatory Research
U.S. Nuclear Regulatory Commission
Washington, DC 20555-001

10. SUPPLEMENTARY NOTES

11. ABSTRACT *(200 words or less)*

A rod ejection accident is a design-basis event for a pressurized water reactor. It is well known that spatial effects play a very important role in this accident. In this study four cases using a model of Three Mile Island Unit 1 are considered: ejection of the central or peripheral control rod at the end of cycle or the beginning of cycle. Calculations were carried out using the BARS neutronic code coupled with the RELAP5/MOD3.2 thermal hydraulic code. This coupled code allows three-dimensional pin-by-pin neutronics and assembly-by-assembly thermal-hydraulics simulation of a transient. The results showed that the major parameters of the accident (the peak power and core energy deposition) were a function of spatial effects. Analysis of the dependence of the peak local fuel enthalpy on spatial effects was performed. Uncertainty analysis was carried out for the central control rod ejection accident at hot zero power conditions. The analysis of uncertainties was performed for the following parameters: local fuel enthalpy, maximum core power, and power pulse width. Calculated results showed that the uncertainty in key safety parameters would be determined to a great extent by the uncertainty in the control rod worth. The effect of initial core power on the above parameters was analyzed using a rod ejection accident starting from 33% of rated power.

12. KEY WORDS/DESCRIPTORS *(List words or phrases that will assist researchers in locating the report.)*

control rod ejection accident
pellet enthalpy
neutron kinetics
PARCS computer code
BARS computer code
spatial effects
uncertainty analysis
code assessment

13. AVAILABILITY STATEMENT

unlimited

14. SECURITY CLASSIFICATION

(This Page)
unclassified

(This Report)
unclassified

15. NUMBER OF PAGES

16. PRICE